THE JOURNAL OF PHYSICAL CHEMISTRY A
A JOURNAL OF THE AMERICAN CHEMICAL SOCIETY

pubs.acs.org/JPCA Article

Mechanism of the Sharpless Epoxidation Reaction: A DFT Study

Robert D. Bach* and H. Bernhard Schlegel

Cite This: J. Phys. Chem. A 2024, 128, 2072−2091 Read Online

ACCESS | Metrics & More | Article Recommendations | Supporting Information

ABSTRACT: The Sharpless reaction is an enantioselective epoxidation of prochiral allylic alcohols that employs a Ti(IV) catalyst formed from titanium tetra(isopropoxide), Ti(O-*i*-Pr)$_4$, diethyl tartrate (DET), and the oxidizing agent *tert*-butyl hydroperoxide. The M06-2X DFT functional with the 6-311+G-(d,p) basis set has been employed to model the structures and energetics of the Sharpless epoxidation reaction. The monomeric tetracoordinate titanium(IV) diethyltartrate is thermodynamically strongly favored to dimerize, producing a pentacoordinate catalyst, [Ti(DET)(O-i-Pr)$_2$]$_2$, that is a more reactive chiral epoxidation catalyst. The rapid ligand exchange reactions needed to generate the "loaded" catalyst and to repeat the overall catalytic cycle have been examined and are found to have activation energies that are much lower than the epoxidation barriers. The transition structures and activation energies for the enantioselective epoxidation of allyl alcohol, *trans*-methyl-allyl alcohol and *trans-tert*-butyl-allyl alcohol with the "loaded" Sharpless catalyst, [Ti$_2$(DET)$_2$(O-*i*-Pr)$_2$-(OAllyl)-(OO*t*-Bu)], are presented. The effect of the C═O···Ti interactions on the activation energies and the significance of the O−C−C═C dihedral angle on the enantioselectivity of the epoxidation reaction are discussed.

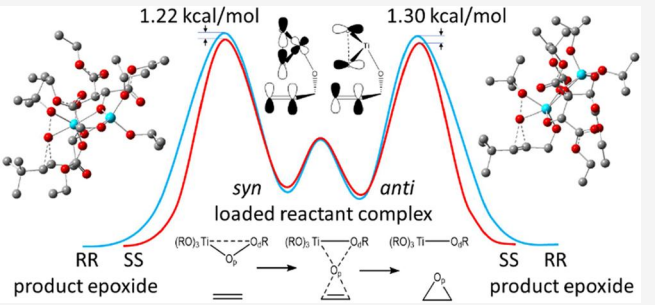

1. INTRODUCTION

The Sharpless epoxidation reaction is an enantioselective reaction for the preparation of 2,3-epoxyalcohols from principally primary and secondary allylic and homoallylic alcohols. Since its initial discovery in 1980,[1] it has evolved into an especially useful technique for the synthesis of numerous chiral starting materials for a variety of pharmaceutical products, antibiotics, and related medicines in both academia and industry.[2,3] The asymmetric synthesis of enantiomerically pure building blocks catalyzed by the formation of only one of the two mirror images of the resulting epoxide was among the first of its kind. This type of chiral catalyst opened up a new field of research that has led to a series of related asymmetric chemical reactions that now strive to mimic enzymatic chemical transformations leading to optically active starting materials. This is the first practical asymmetric synthesis by which epoxides of a single handedness could be selectively produced in the laboratory even though nature does this routinely. Perhaps more importantly, this reaction sequence demonstrated the capacity to duplicate what nature does consistently in comparable enzymatic processes. It was recognized early on that the titanium catalyst, Ti(O-i-Pr)$_4$, existed in dimeric form, but the initial structure proposed was a ten-membered ring with a pentacoordinate transition state (TS) for asymmetric epoxidation.[4] However, it was also known that other related titanium tartrate complexes tend to exist as a cyclic 4-membered structure with two adjacent Ti−O−Ti bridges. This led Sharpless and co-workers[5] to the suggestion that the active epoxidation catalyst was a tightly bound dimeric hexacoordinate structure as is now universally recognized. More recently, NMR data[4] and X-ray studies[6] have provided strong support for the proposed Sharpless dimer as the active catalyst.

After considerable development, the most commonly applied version of the reaction employs a titanium tetraalkoxide, a tartrate ester as the chiral auxiliary, and an allylic alcohol as the substrate.[7] Most typically, *tert*-butyl hydroperoxide (TBHP) serves as the oxidizing agent because a sterically hindered oxidant is essential for high enantioselectivity and the solvent of choice is generally methylene chloride. The conversion of this initial catalytic reagent, derived from the ligand exchange of titanium(IV) isopropoxide [Ti(O-i-Pr)$_4$] with diethyl tartrate (DET), produces the chiral reagent [Ti(DET)(O-i-Pr)$_2$] that is now poised to achieve excellent enantioselective epoxidation with remarkable consistency on a wide variety of allylic alcohol substrates [Ti$_2$(DET)$_2$ (O-i-Pr)$_2$-(OAllyl)-(OO*t*-Bu)]. The Sharpless epoxidation is unique in that it converts a prochiral allylic alcohol into the corresponding chiral epoxide with a high enantiomeric excess (% ee).

Received: December 29, 2023
Revised: February 20, 2024
Accepted: February 20, 2024
Published: March 7, 2024

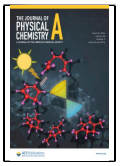

https://doi.org/10.1021/acs.jpca.3c08476
J. Phys. Chem. A 2024, 128, 2072−2091

We have recently reported a systematic study that compares the mechanism of oxygen atom transfer for several well-established oxidation reactions.[8] A comparison of the mechanism for these classical peroxyacid epoxidation of alkenes and hydrocarbon oxidation with hydroperoxides shows that the Ti(IV)-catalyzed epoxidation proceeds by an entirely different mechanism. As opposed to a 1,4 or 1,2 hydrogen atom shift involved in the aforementioned reactions, we have described the molecular motion in Ti(IV)-catalyzed epoxidations as a 1,3-rearrangement of the *tert*-butoxide group in concert with the oxygen proximal to the Ti transferred to the alkene substrate. This rational provides an explanation for the relatively low calculated barrier for Ti(IV) catalyst epoxidation ($\Delta H^{\ddagger}$ = 15.4 kcal/mol)[8] despite the high Ti−O−O bond dissociation enthalpy for this Ti-bound peroxide (60 kcal/mol).[9] The O−O bond dissociation involves breaking both the O−O bond (1.44 Å) and the secondary η^2-Ti−O bond (2.10 Å). In contrast, the rate-limiting oxygen transfer step in epoxidation involves cleavage of the primary Ti−O bond in concert with a shortening of the secondary η^2-Ti−O bond attending the 1,3-OC$(CH_3)_3$ ligand migration, thereby reducing the activation barrier. It was recognized very early in the development of the Sharpless reaction that in the TS the OOR ligand is bound covalently to the Ti atom, thereby activating the oxygen proximal to the metal to transfer to the substrate.[10] The nuclear event for a 1,3-rearrangement of the alkoxide ligand in a titanium hydroperoxide to the Ti center in concert with concomitant oxygen atom transfer of the proximal oxygen to the C=C bond of the substrate is presented in eq 1.[11]

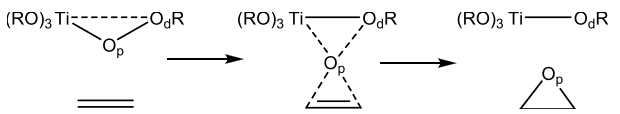

We now report a series of transition structures (TSs) for the epoxidation of Ti-bound allyl alcohols with the dimeric fully "loaded" Ti(IV) catalyst that has been customarily used in the Sharpless epoxidation.[1] We describe the intricate mechanistic details of the oxygen atom transfer step and the origin of the high enantioselectivities that have been observed by the experimental community for four decades.

2. COMPUTATIONAL METHODS

The density functional theory (DFT) calculations were performed with Gaussian 16.[12] The minima and transition structures involving oxygen atom transfer presented in the figures and discussed in the text were fully optimized[13] using the M06-2X density functional[14] with the 6-311+G(d,p) basis set unless otherwise noted. Transition states for epoxidation have been tested for wave function stability and showed no singlet or triplet diradical character. Spin−orbit contributions are expected to be very small because Ti(IV) is formally d^0 with no occupied d orbitals. We have found that the M06-2X functional provided very good O−O bond dissociation enthalpies, while the B3LYP functional[15,16] underestimates the energetics of O−O bond cleavage.[9,17] Another advantage of the M06-2X functional is that it is parametrized to reproduce the dispersion energy without adding empirical dispersion corrections.[18] This is useful because of the number of secondary nonbonding interactions and relatively close van der Waals interactions involved in these complex structures. The numerous nonbonding interactions necessitated that we initiate preliminary calculations for the TSs where initially the O−O and the two epoxide C−O bond distances were frozen. The Hessian was computed, and the constrained optimization was allowed to proceed for 20 steps. This procedure typically had to be repeated several times with the frozen bond distances updated each time before removal of constraints and full geometry optimization. Solvent corrections were calculated initially with the default polarizable continuum model in the Gaussian code (IEFPCM) using this same basis set. However, for the section on the *trans*-methyl-allyl and the more sterically demanding *tert*-butyl allylic alcohol section, we used the SMD variant that was parametrized specifically for M05-2X/6-31+G** and has been applied extensively with the M06-2X density functional.[19] Frequency calculations were carried out on all fully optimized structures at this same level to verify that they are either minima or first-order saddle points (TSs). Cartesian coordinates, total SCF energies, enthalpies at 298 K, and Gibbs free energies at 298 K are listed in the Supporting Information. Relative Gibbs free energies are given in the figures.

A major problem in determining the optimized geometries with the relatively small energy differences of these structures is the numerous C−H bonding interactions with the carbonyl oxygens of the CO_2Et groups. In each of the structures, one of the ester carbonyl oxygens also forms a relatively strong C=O···Ti bond that has a stabilizing action and influences the overall reaction energetics. The dihedral angles involving the ester functionality can shift quite easily and can require many gradient cycles to optimize the displacements after the forces have converged. The secondary H-bonding interactions at ≈2.5 Å can add up to several kcal/mol and make it difficult to arrive at consistent minimum energy structures. The procedure we typically practice is to take the lowest energy fully optimized structure for one conformer and simply rotate about the O−C−C=C dihedral angle of the allyl alcohol to get the starting geometry that presents the opposing C=C stereoface without altering any of the CO_2Et dihedral angles.

3. RESULTS AND DISCUSSION

3.1. Background. In a recent study,[9] we reported that O−O bond dissociation enthalpies (BDEs) for a series of peroxides with the M06-2X density functional provided O−O BDEs within 1−2 kcal/mol of the values obtained with the CBS-QB3[20] and CBS-APNO higher-level composite methods.[21] We have also shown that the M06-2X functional provides comparable accuracy for BDEs of the N−O bond.[17] These findings prompted us to use the M06-2X functional in the current study since O−O bond cleavage is the key step in the reaction. This is especially relevant since the catalyst in the Sharpless reaction employs a Ti(IV) *tert*-butyl hydroperoxide oxidant, and we found that its O−O BDE was much higher than might have been anticipated. While the O−O BDE of a generic peroxide has now been ascribed a bond energy of ca. 45 kcal/mol,[9] the O−O BDE approaches 60 kcal/mol (CBS-QB3) for a titanium peroxide ($(RO)_3$TiO-OC$(CH_3)_3$) that models the Sharpless catalyst.

Since the introduction of the Sharpless reaction in 1980,[1] there have been a great many experimental papers published on the mechanism of metal-catalyzed oxidation but surprisingly few theoretical papers on an epoxidation reaction of this importance. The earliest attempt to describe the mechanism of this reaction was an insightful frontier molecular orbital theory study, based upon extended Huckel's theory, by Jorgensen,

https://doi.org/10.1021/acs.jpca.3c08476
J. Phys. Chem. A 2024, 128, 2072−2091

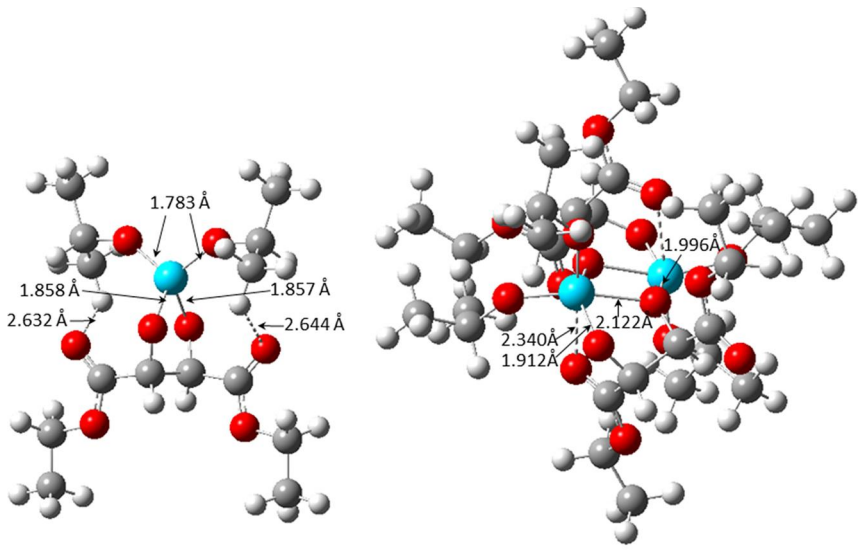

Figure 1. Dimerization of Ti(IV)-(*R*,*R*)-diethyl tartrate-diisopropoxide.

Wheeler, and Hoffmann.[22] They suggested that the orientation and reactivity of the alkene C═C in the allyl alcohol could be traced to the interaction of the peroxygen lone-pair and the π^* orbital of the alkene and to the interaction of the titanium−peroxygen antibonding orbital with the π orbital of the alkene. In 1994, Wu and Lai[23] reported a TS for the trihydroxytitanium hydroperoxide ((HO_3)Ti(IV)OOH) epoxidation of ethylene and an activation energy of 10.7 kcal/mol. This investigation was extended in a DFT study of the Sharpless epoxidation that included the dimeric catalyst with allyl alcohol (prop-2-en-ol) and *tert*-butyl hydroperoxide (TBHP).[24] Because of the overall size of the catalyst system, geometry optimization was limited to BLYP/3-21G with energies calculated with the HW3 basis (equivalent to the 6-31G* basis set). DFT studies by Root et al.[25] on the origin of the reactivity of titanium hydroperoxide catalysts in the epoxidation of ethylene were subsequently reported. Although many novel mechanistic features of alkene epoxidation with Ti-containing polyoxometalates have been reported,[26−28] none of these studies, based upon H_2O_2 as the oxidative reagent, can serve as a model for the Sharpless epoxidation. The rate-limiting η^2-O−O bond cleavage step involves migration of the hydroxy anion to the Ti center and, in the absence of the essential hindered alkyl hydroperoxide, this catalyst cannot provide any steric role in the enantioselectivity of the resulting epoxide. For this reason, the peroxide of choice for the Sharpless epoxidation is TBHP.[1]

In the 44 years since the Sharpless reaction was reported,[1] there have been only three reports of a TS for a Ti(IV)-catalyzed epoxidation using an alkyl hydroperoxide. In 2002, Adam, Jiang, and co-workers[29] used DFT calculations (B3LYP/6-31+G(d,p)) to study the diastereoselective epoxidation of a series of methyl-substituted allylic alcohols. However, in this series of bimolecular epoxidation reactions, the simplified $Ti(OH)_4/CH_3OOH$ complex was used as a model for the Sharpless oxidant $Ti(O\text{-}i\text{-}Pr)_4$/*t*-BuOOH. A few years ago, we reported[11] a series of TSs for the epoxidation of Ti-bound allyl alcohol where the Ti(IV) catalyst is composed of the bidentate(R,R)-(+)-diethyl tartrate chiral auxiliary and *tert*-butyl hydroperoxide that are the basic reactants in the Sharpless epoxidation.[1] More recently, Freindorf and Kraka[30] have reported the Ti(IV)-catalyzed methyl hydroperoxide epoxidation of allyl alcohol employing an amide modification of the diethyl tartrate. This study used the unified reaction valley approach (URVA) and local mode analysis to describe the intricate motions and energetics of bond making of the oxygen transfer step. This study suggested that the major effect of the Ti(IV) catalyst is the weakening of the O−O bond of the peroxide upon coordination at the metal atom.

3.2. Dimerization Step. Our recent paper[11] reported the first calculations on the dimerization of the monomeric catalyst producing Ti(IV)-(*R*,*R*)-diethyltartrate-diisopropoxide. These B3LYP DFT calculations provided additional evidence in support of the idea that the dimeric form of the catalyst is essential in order to create sufficient steric congestion to result in an enantiomeric excess in the oxygen transfer step. In general, the Sharpless epoxidation yields epoxides with a high degree of enantiomer purity. However, upon inspection of the monomeric catalyst (Figure 1), it was immediately obvious that the two chiral centers cannot exert any steric influence upon the enantiomeric selectivity of the epoxide product because they are too far removed from the active Ti reaction center containing the allylic alcohol and Ti(IV) peroxide. With this series of single Ti-centered epoxidations of allyl alcohol, we noted a substantial decrease in activation energy ($\Delta\Delta G^{\ddagger}$ = 7.54 kcal/mol) for Ti(IV)-catalyzed epoxidation when we change from a tetracoordinate monomeric catalyst to a pentacoordinate Ti environment, which is present in the dimeric catalyst. Finally, the energy for dimerization of the monomeric catalyst (B3LYP) was ΔG = −11.28 kcal/mol, providing a reason for dimerization.[11]

In an effort to provide dimerization data that is consistent with values given in the present study, we re-examined the dimerization reaction with the M06-2X DFT functional. The carbonyl groups in the monomer form two relatively strong H-bonds (2.632 and 2.644 Å) to one of the hydrogens of the adjoining isopropyl group (Figure 1). In addition, the C═O groups have a relatively weak interaction with the Ti center

https://doi.org/10.1021/acs.jpca.3c08476
J. Phys. Chem. A 2024, 128, 2072−2091

(3.32 and 3.28 Å). Both C═O groups are nearly *syn* to each other (O═C···C═O dihedral angle = 25.2°). The five-membered ring containing the Ti atom is slightly puckered with a O−C−C−O dihedral angle of 41.6°. The bond angle between the two oxygens in the $Ti(O\text{-}i\text{-}Pr)_2$ fragment is 110.8°. The other TiO_2 angle formed between the two diolate oxygens is 84.2°. The dihedral angle between the $Ti(O\text{-}i\text{-}Pr)_2$ and $Ti(O{-}CH)_2$ planes is not quite orthogonal (82.0°). The dihedral angle of the ethyl groups in the ester relative to the C═O is *anti* as usual, but once dimerized, the ethyl groups usually become distorted because of steric interactions as we note below.

The monomer has a tetracoordinate Ti local environment that can achieve a much more stable structure through dimerization to form a pentacoordinate dimer. The dimeric form, $[Ti(DET)(O\text{-}i\text{-}Pr)_2]_2$, has a bridged arrangement of the tartrate bidentate ligand. The cyclic 4-membered array in the dimer is essentially planar with a Ti−O−Ti-O dihedral angle of 2.6°. The distance between the two Ti atoms in this four-membered ring is 3.329 Å, and the opposing oxygen atoms are 2.426 Å apart. In the dimer, one of the tartrate diol oxygens has a somewhat shorter O−Ti atom bond (1.9 Å), while the bridging oxygen bonding to both Ti atoms is about 2.1 Å. The O−Ti−O angles in the $Ti(O\text{-}i\text{-}Pr)_2$ fragments are 97.1° and 99.5°. This is a somewhat different bonding arrangement than we reported earlier[11] with the B3LYP functional. This tighter bonding arrangement and the fact that the M06-2X functional provides better treatment of dispersion interaction between the secondary nonbonding interactions of the highly encumbered ester groups accounts for its greater dimerization energy (ΔG = −34.27 kcal/mol), thereby providing a substantial impetus for dimerization.

The core of the dimer has pseudo-C_2 symmetry, but the four CO_2Et functional groups in the dimer can be arranged about the Ti_2O_2 cyclic array with a number of different dihedral angles with respect to each other. Two of the ester groups of the dimer shown in Figure 1 have strong bonding interactions between the carbonyl oxygen atom and a Ti atom (2.340 and 2.405 Å) that contribute to the stabilization of the dimer. For example, we have found that the interaction of the epoxide product oxygen with the Ti center at a distance of 2.29 Å can provide as much as 12 kcal/mol to the overall stabilization.[11] The other two carbonyl groups are too far from the Ti atoms to contribute significantly to the stabilization of the dimer.

A combined theoretical and mass spectral analysis of the Sharpless Ti(IV) dimeric structure has been reported[31] that suggested the possibility of an asymmetric species with the two tartrates coordinated to a single Ti atom, while the other Ti center is coordinated by three labile alkoxides (methoxide). Based upon the above considerations, we feel that the asymmetric dimer, with only one Ti center involved, does not have the intrinsic electronic and steric properties to create an environment that surrounds the reaction site and can provide a chiral epoxide. This asymmetric dimeric form was also shown by B3LYP/6-31+G(d,p) calculations to be slightly higher in energy (2.75 kcal/mol) than the corresponding symmetric methoxide dimer. The strong driving force for dimerization (34 kcal/mol) yields a highly hindered local environment of a "loaded" dimeric catalyst that can play a major role in the enantiomeric selectivity in the epoxidation step.

3.3. "Loaded" Catalyst Structure. After the formation of the Ti-tartrate dimer, a statistical mixture of Ti species can arise from the exchange of the isopropoxide ligands of the dimeric complex with the chosen hydroperoxide, typically *tert*-butyl hydroperoxide, and the substrate allylic alcohol.[7] This is a very rapid reversible exchange reaction because Ti(O-iPr) ligands can exchange much faster than the tartrate ligand since the bidentate diol has a much higher binding constant than the monodentate alcohol as discussed below.

3.3.1. Syn and Anti Structures. When exchanging ligands on the $[Ti(DET)(O\text{-}i\text{-}Pr)_2]$ group, the allylic alcohol can approach the dimeric structure either in a manner that is *syn* to the CO_2Et group in ring A or in the opposite or inverted direction that is *anti* to the CO_2Et group in ring A (Figure 2).

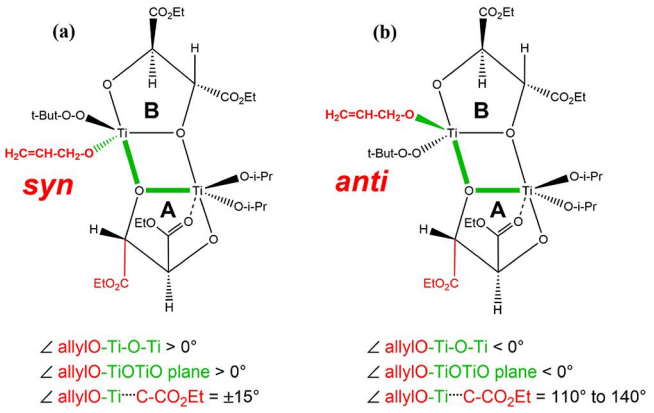

Figure 2. Loaded catalysts for the *syn* and *anti* structures, characterized by the dihedral angle of the allyl-O group, the out-of-plane angle between the allyl-O group and TiOTiO plane, and the dihedral angle between the allyl-O group and the CO_2Et group in ring A.

Ring B may be distinguished from ring A in that it has both oxygens of the tartrate diol bound to Ti with the allylic alcohol and the peroxide, while ring A has only one oxygen atom bound to this Ti. The absolute configuration of the CO_2Et tartrate ligands in both rings is (2*R*,3*R*), and the configuration of the allylic alcohol is specified by its *syn*/*anti* relationship relative to the adjacent CO_2Et group in ring A. By definition, the *anti*-configuration has the allylic alcohol *anti* to that CO_2Et group and *tert*-But-OO ligand *syn* to it. An alternate way of identifying the *syn*/*anti* conformation is to look at the Ti−O−Ti-Oallyl dihedral angle (green bonds in Figure 2) or the out-of-plane angle that the O-allyl group makes with the Ti−O−Ti plane. A value greater than 0° means that the O-allyl moiety is in a *syn* position and a value less than 0° places the O-allyl in an *anti*-position, as shown in Figure 2.

It is now well-established that the Ti-bound *tert*-butyl peroxide is potentially a bidentate ligand because in addition to the primary Ti-peroxygen bond, there is a somewhat longer secondary Ti−O bond in the η^2 coordinated peroxide that plays a major role in the oxygen transfer step. The calculated η^2-coordination of the peroxide moiety of alkyl hydroperoxides has been confirmed by an X-ray study.[32] The resulting epoxide in this epoxidation reaction can potentially arise from a TS involving either *syn* or *anti* loaded catalysts. In addition, rotation about the O−C−C═C dihedral angle in the allylic alcohol gives rise to two additional TSs which further complicate this overall reaction scheme. The accompanying $Ti(O\text{-}i\text{-}Pr)_2$ fragment in the dimeric form is not simply a spectator group but plays an essential role in providing the local steric environment that is responsible for sterically

https://doi.org/10.1021/acs.jpca.3c08476
J. Phys. Chem. A 2024, 128, 2072−2091

restricting the approach to the active reaction template. These steric interactions provide the geometric arrangement responsible for the electronic requirements of the TS and the steric environment ensuring the desired enantioselectivity. Additionally, the pseudo C_2-symmetry can potentially reduce the number of pathways for the incoming electrophilic oxygen to approach the C═C bond and hence the number of stereoisomers produced.

It has generally been assumed[7,33] that a relatively small allylic alcohol approaches the dimeric complex in a manner that is *syn* to the adjacent CO_2Et group in ring A but *anti* to the ester group in ring B, as shown in Figure 2a. We will note later that the allyl alcohol and substituted allylic alcohols like *trans*-methyl and *trans-tert*-butyl-allylic alcohol can exchange from the opposite direction and the exchanging alcohol resides *anti* to the CO_2Et group in ring A, as shown in Figure 2b.

3.3.2. Energetics of the C═O···Ti Interaction. As we reported earlier,[11] the Ti···O interaction in the epoxide product of a Ti(IV) epoxidation reaction had a stabilization energy of ≈12 kcal/mol. As we discuss below, the C═O group of the axial CO_2Et group in ring A (Figure 2) interacts strongly with one of the Ti centers in the dimeric loaded catalyst and plays a major role in determining the overall stability of the complex. To obtain a more quantitative estimate of the magnitude of the complexation energies, $Ti(OCH_3)$-$(OCH_2CH_2O)CH_2CH_2CO_2Et$ was used to model the ground state with and without Ti···O interactions (Figure 3). The C═O moiety is tethered to the Ti center to approximate the local environment in the loaded catalyst system. In the extended geometry (ΔG_{rel} = 0.0), the OCH_2-CH_2C═O dihedral angle was constrained to 110° so that the carbonyl oxygen and ester oxygens were 4.6 and 5.7 Å away from the Ti center. When this geometric constraint was released, with geometry optimization, the ester oxygen had a Ti···O bond distance of 2.304 Å and the Gibbs free energy of the alcohol oxygen Ti-complex was reduced by 10.26 kcal/mol. The magnitude of this stabilization was quite similar to what we had observed (12 kcal/mol) for the interaction of a Ti center with an epoxide oxygen.[11] However, a lower energy conformation was observed, where the carbonyl oxygen Ti interaction had a Ti···O distance of 2.182 Å and exhibited a surprising stabilization energy of 14.28 kcal/mol. These data point out one of the most serious problems with locating the most stable geometries for these very complex loaded catalyst structures.

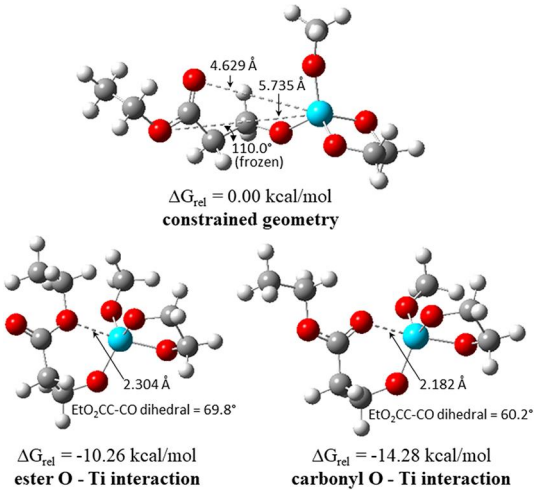

Figure 3. Relative stabilization free energies for ester oxygen and carbonyl oxygen interacting with the Ti center.

3.4. Epoxidation Step. For a majority of the Sharpless epoxidation reactions, the enantioselectivity is determined by a $\Delta\Delta G^{\ddagger}$ that is 2 kcal/mol or less (2.00 kcal/mol corresponds to 97% ee). Consequently, the very subtle structural differences in the two competing TSs may not be readily discernible upon visual comparison. Our mechanistic blueprint is to identify the key electronic perturbation properties of the TSs that serve to describe the more energetically responsive molecular changes that contribute to the competing activation barriers. First, the electrophilic oxygen of the incoming peroxide should approach the center of the C═C π-bond in as nearly a linear manner as possible in the oxygen transfer step. This direct approach can be somewhat impeded by local steric interactions.

Second, the planes of R-C═C-R and Ti−O−O of the Ti(IV) catalyst should be perpendicular to each other in order to maximize the interaction of the lone pair of electrons of the incoming electrophilic oxygen atom with the π^* orbital of the alkene. Third, when the plane containing the C═C bond and the transferring oxygen makes a 90° angle with the plane of the peroxyacid, the orientation is defined as spiro.[34−36] In this orientation, the oxygen atom lone pair has the proper orbital symmetry to overlap with the alkene π^* orbital. We have estimated[11] that this interaction is ≈2.6 kcal/mol when compared to a planar epoxidation TS where the angle between the two planes is constrained to be 0°.

Proceeding along the reaction coordinate in the TS, the angle between the C−O−C plane of the developing epoxide (i.e., the C═C π-orbital plane) and that of the Ti(IV)−O-O plane can change dramatically as the O−C−C═C dihedral angle shifts to place the C═C in closer proximity to the transferring oxygen atom. Deviation of this angle from 90° will provide a measure of the sterically imposed distortion of the bonding interactions between the two approaching reagents in the TS and hence its deviation from a pure spiro TS. As noted above, this interaction is ≈2.6 kcal/mol when compared to a planar bimolecular epoxidation TS where the angle between

Scheme 1. Peroxygen Lone-Pair-π^* and Antibonding Ti-d-Orbital−Oxygen p-Orbital−π-Orbital HOMO−LUMO Orbital Interactions Involved in Ti(IV)-Catalyzed Epoxidation

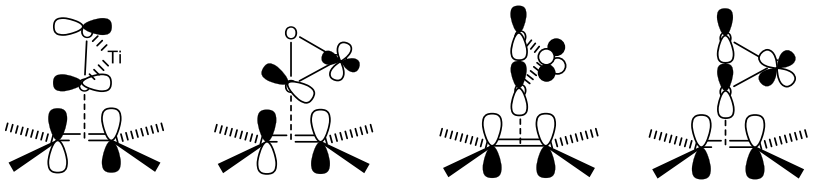

https://doi.org/10.1021/acs.jpca.3c08476
J. Phys. Chem. A 2024, 128, 2072−2091

the two planes is constrained to be zero degrees.[11] This can have an impact upon the respective lengths of the two developing C−O bond lengths in the TS. This is particularly relevant to the activation energy because the average bond dissociation energy of a generic single C−O bond is ≈80 kcal/mol. We can estimate[11] that an asymmetric approach of the oxygen to the C═C bond, when elongating the C−O bond in dimethyl ether by as little as 0.1 Å, can alter the enthalpy of the system by as much as 2.7 kcal/mol. Thus, the energetics of the bond-making step can be competitive with the oft-quoted lone-pair-π^* interaction.[35]

The oxygen atom transfer step in the TS for this Ti(IV)-catalyzed epoxidation reaction is facilitated by HOMO−LUMO interactions.[22] The "culprit" atom, in the epoxidation reaction, is the peroxygen atom because it is directly involved in both the bond-making and bond-breaking steps in the TS. Historically, we have paid much more attention to the atom motion involved in the bond making step than in the issues required to cleave the Ti−O bond (Scheme 1).

Epoxidation reactions are typically carried out at room temperature or lower, so the cleavage of the very strong Ti−O bond must be induced by some electronic event. As the peroxygen atom approaches the electrons of the alkene π-orbital donor, it interacts with an acceptor antibonding titanium d-orbital−peroxygen p-orbital combination that induces a weakening of the Ti−O bond in concert with it developing a bonding interaction with the C═C bond.[22] The bond-making step, which produces the two C−O bonds in the epoxide, involves a bonding interaction between the peroxygen atom lone pair of electrons with the alkene π^* orbital that serves as the acceptor orbital. This favorable HOMO−LUMO interaction, by symmetry, favors a spiro orientation of the C═C portion of the allylic alcohol with the titanium peroxygen bond.

3.4.1. Alkene Epoxidation with Peroxyacid. We initiate this part of the study by including the peroxyacid epoxidation of a simple alkene as an exemplary epoxidation reaction because of its historical perspective.[37,38] There have been numerous theoretical studies on this relatively simple oxygen atom transfer[8] that on comparison can serve to exemplify the more complex epoxidation mechanisms involving Ti(IV) catalysts.[11] We recently described the bimolecular epoxidation of E-2-butene with peroxyacetic acid (Figure 4). The calculated free energy of activation, $\Delta G^{\ddagger}$ = 34.46 kcal/mol,[11] is considerably higher than the activation enthalpy, $\Delta H^{\ddagger}$ = 22.60 kcal/mol, for this bimolecular epoxidation reaction. This is because of the loss of translational and rotational degrees of freedom that accompanies the formation of the transition state from separated reactants in a bimolecular reaction. The Gibbs free energy barriers can be increased further when the TS is highly ordered and the two bonding entities are required to be in a specific orientation. In the spiro-TS, the angle between the incoming O−O bond and the midpoint of the C═C bond is essentially linear (179.4°) for this unencumbered approach of the two reactants. In addition, the angles between the peroxyacid C−O−O plane and the C−O−C and C═C−H planes of the developing epoxide are 90° and 95.4°, respectively, supporting a spiro orientation of the interacting frontier orbitals, as delineated in Figure 4 (top).

The HOMO−LUMO interaction of the oxygen lone-pair with the symmetry-allowed alkene π^* orbital is involved in the C−O bond-making step. We also show an orbital interaction that is barely mentioned in epoxidation reactions, the

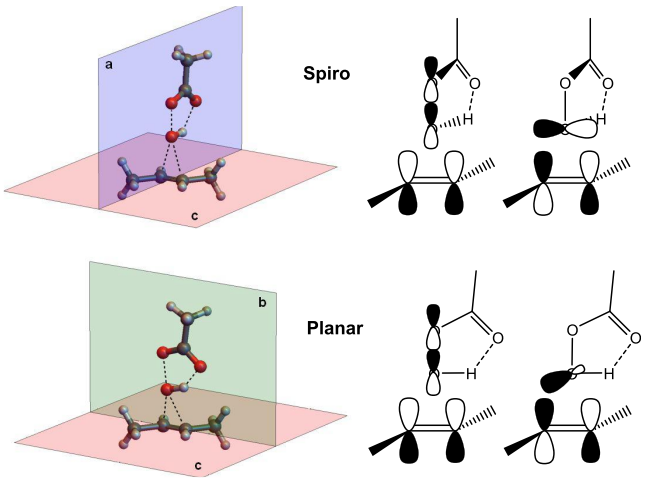

Figure 4. Interactions between oxygen and alkene π and π^* orbitals in transition states for the peroxyacetic acid epoxidation of E-2-butene in the spiro orientation (top, peroxyacid C−O−O in the *a* plane) and the planar orientation (bottom, peroxyacid C−O−O in the *b* plane).

interaction of the alkene HOMO π orbital with the electrophilic oxygen O−O σ^* orbital that initiates the O−O bond cleavage in concert with the 1,4-hydrogen shift to the carbonyl oxygen that consummates oxirane formation.

We also present the planar-TS where the geometry of the peroxyacid and the C═C are constrained to be in a planar relationship throughout the oxygen transfer step where the sp^2-hybridized oxygen lone pair can interact with the π^* orbital (Figure 4, bottom). The computed enthalpy barrier for the planar peroxyacid TS ($\Delta H^{\ddagger}$ = 24.16 kcal/mol)[11] is 1.56 kcal/mol greater than that of the spiro TS. As we note below, the Ti(IV)-catalyzed intramolecular reactions in the Sharpless epoxidation can have transition states with distorted spiro and planar geometries as a consequence of the influence of the different O−C−C═C dihedral angles of the substrate allylic alcohols in the TS. The orbital distortions in the TS play a major role in determining the spiro vs planar orientation in the rate-limiting oxygen transfer step.

3.5. Detailed Mechanism for Alkene Epoxidation with a Model Ti(IV) Catalyst. The intricate mechanistic nuances of the Sharpless epoxidation can be obscured by the sheer size and steric bulk of the overall hexacoordinate dimeric catalytic system. We can more closely examine the important individual mechanistic steps of this epoxidation reaction by using a monomeric pentacoordinate titanium(IV) hydroperoxide catalyst. We have included an ethylene glycol diolate to model the bidentate chiral auxiliary. In **GS-1** (Figure 5), the allylic alcohol has a O−C−C═C dihedral angle of −123.1°

and the proximal oxygen of the *tert*-butyl peroxide is 5.2 Å away from the terminal C═C carbon. This will require a lot of O−C−C═C bond rotation in the TS to place the C═C face in its proper juxtaposition for oxygen atom transfer. As previously described,[11] the oxygen atom transfer step involves a 1,3-rearrangement of the distal oxygen of the *tert*-butoxide resulting in the $OC(CH_3)_3$ ligand being strongly bound to the titanium center in epoxide-**1**.

The atom motion involved in the 1,3-migration of the *tert*-butoxide group is shown in Figure 5. In **GS-1**, the Ti−O bond proximal to the $OOC(CH_3)_3$ ligand is 1.884 Å, while the distal oxygen of the η^2-coordinated peroxide has a somewhat longer Ti−O bond distance of 2.135 Å. As we observe the migration

https://doi.org/10.1021/acs.jpca.3c08476
J. Phys. Chem. A 2024, 128, 2072−2091

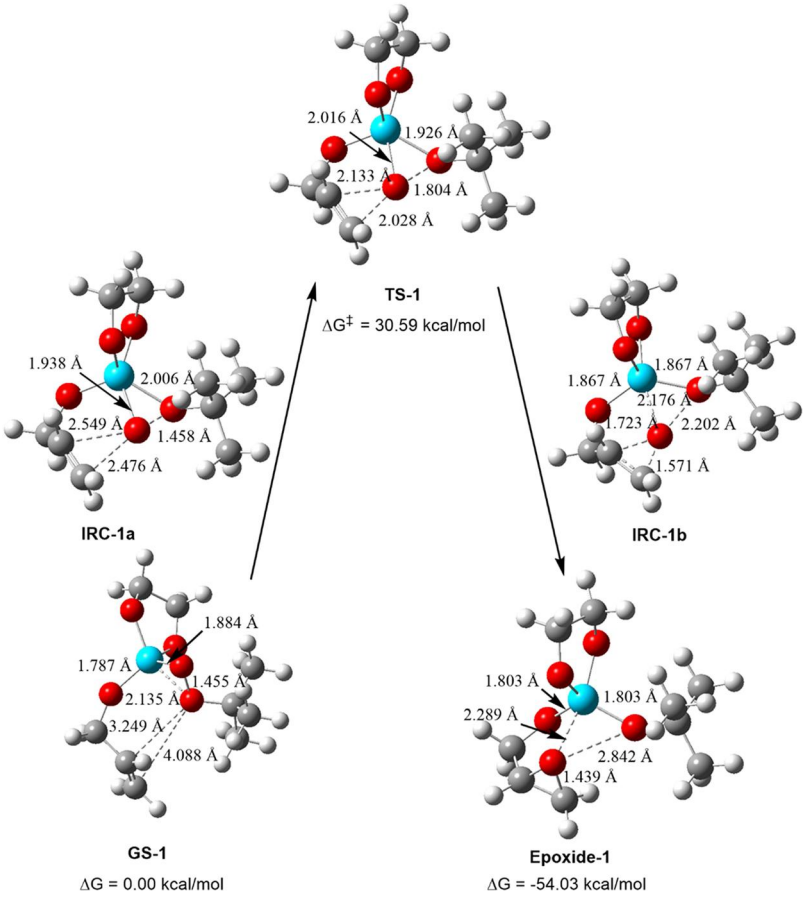

Figure 5. Molecular motions involved in the monomeric Ti(IV)-catalyzed epoxidation of allyl alcohol.

of the $OC(CH_3)_3$ ligand, the distal Ti−O bond contracts to 2.006 Å in **IRC-1a** and to 1.926 Å in **TS-1** (Figure 5). On the pathway from **GS-1** to **TS-1**, the energy has increased by 38% at **IRC-1a** and the $OC(CH_3)_3$ migration is nearly completed (compare to the Ti−O distance of 1.803 Å in **Epoxide-1**). In concert with this motion, the Ti−O bond of the proximal transferring oxygen has decreased to 2.016 Å in **TS-1** and has a Ti−O bond distance of 2.289 Å in **Epoxide-1**. In terms of energy, **IRC-1b** is 50% of the way between the energies of **TS-1** and **Epoxide-1**. The secondary η^2-Ti−O bond in these Ti(IV) peroxides is an integral part of the overall 1,3-alkoxide migration. We have estimated the bond strength of the η^2-Ti−O bond (2.13 Å) in **GS-1** by constraining the Ti−O−O bond angle (78.1°) to that in *tert*-butyl hydroxide (109.1°), thereby increasing the η^2-Ti−O bond length to 2.679 Å and the Gibbs free energy of the Ti(IV) peroxide by 5.13 kcal/mol.

In the absence of steric interactions, the orientation of the incoming peroxide oxygen can be restricted to one that accommodates a near linear attack where the midpoint of the C═C bond is aligned with the O−O bond axis to produce a near linear arrangement in **TS-1** (166.6°). The negative O−C−C═C dihedral angle, which would produce the S-epoxide, contracts somewhat to −114.7° in **TS-1** (Figure 5). The O−O-*tert*-butyl angle is 114.9° and the Ti−O-*tert*-butyl angle is 137.1°. The dihedral angle between the R-C═C-R plane and the TiO_2 plane is 79.3°. The developing angle between the C−O−C plane of the epoxide product being formed and the TiOO plane should approach 90° for a spiro-TS or near 0° for a planar TS as described above. Since this angle is only 9.6° in **TS-1**, it is very close to a planar TS.

The majority of the heavy atom motion described by the IRC is rotation of the TiO−CC═C allylic alcohol dihedral angle from 12.4° in the GS to 26.1° in the TS. This motion serves to place the terminal C atom of the C═C much closer to the electrophilic oxygen (5.25 Å → 2.03 Å). The O−O bond is not elongated until very late along the reaction path. In the GS, the O−O bond is 1.44 Å, and by **IRC-1a**, the O−O bond is still only 1.46 Å and the O−C bond to the terminal carbon is at 2.48 Å. The opposite is true for the bond-making steps attending oxygen atom transfer where the oxygen is transferred in only a few steps past the TS and most of the reaction coordinate is composed of torsion about the OC−C(O)C epoxide bond to bring the epoxide oxygen into bonding distance for a secondary bonding interaction with the Ti atom. Thus, most of the activation energy is composed of the atom motions leading up to and including the O−O bond cleavage. We have estimated that the strength of this intramolecular Ti···O bond in the epoxide could be ≈12 kcal/mol, so this could be largely responsible for the rotational effect late on the reaction coordinate.[10] This torsion also provides a rational for why the aforementioned C−O−C/TiOO planes are approaching a planar TS. This is a highly exothermic reaction with a Gibbs free energy of reaction (ΔG = −54.03 kcal/mol) for **Epoxide-1** formation that is increased by this relatively strong intramolecular Ti···O bond to the epoxide oxygen. The barrier for epoxidation is $\Delta G^{\ddagger}$ = 30.59 kcal/mol. For the sake of comparison, the same epoxidation TS but with the opposite C═C face exposed (dihedral angle O−C−C═C = 33.9°) had a very similar geometry and Gibbs free energy of activation $\Delta G^{\ddagger}$ = 30.83.[11] Thus, in the absence

https://doi.org/10.1021/acs.jpca.3c08476
J. Phys. Chem. A 2024, 128, 2072−2091

of the steric influence of diethyl tartrates in their dimeric form, the Ti(IV)-catalyzed epoxidation TSs exhibit geometries that are very close in structure and seem to be controlled largely by electronic interactions. However, the TS producing the 2*R*,2*R*-epoxide, with a positive dihedral angle, is closer to a spiro TS.

3.5.1. Epoxidation of Allylic Alcohol. The ground-state free energies and structures for the loaded catalyst involved in the epoxidation of allyl alcohol (prop-2-en-1-ol) are shown in Table 1. The alcohol can be oriented *syn* or *anti* to the adjacent

Table 1. Activation Parameters for the Epoxidation of Allyl Alcohol

structure	∠O−C−C=C°	Ti−O−Ti-O-allyl dihedral	ΔG_{rel}	$\Delta G^{\ddagger}$ (GS-*n* →TS-*n*)	% epoxide[a]
GS-2a *syn*	131.0	114.3	1.62		
GS-2b *syn*	−127.4	97.1	2.43		
GS-2c *anti*	124.2	−122.0	0.00		
GS-2d *anti*	−124.0	−124.1	0.62		
TS-2a *syn*	36.1	104.5	27.97	26.35	10.8% R
TS-2b *syn*	−106.2	100.4	26.72	24.29	89.2% S
TS-2c *anti*	31.9	−114.1	27.78	27.78	34.9% R
TS-2d *anti*	−105.7	−115.1	27.41	26.79	65.1% S

[a]For no interconversion between *syn* and *anti*; when *syn*/*anti* interconversion is faster than epoxidation, the calculated yield of the epoxide is 18.0% R and 82.0% S corresponding to 64.0% ee.

CO_2Et group in ring A (Figure 2). A O−C−C=C dihedral angle greater than zero in the loaded catalyst exposes the *Si* face of the C=C to the electrophilic oxygen to afford the 2R-epoxide in accordance with the Sharpless mnemonic[1] (Figure 6), while the O−C−C=C dihedral angle less than zero yields the 2S-epoxide.

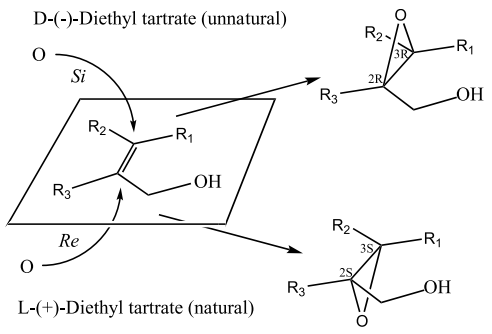

Figure 6. Schematic that predicts the chirality of the epoxide product in the Sharpless epoxidation.

The structures of the *syn* ground states are shown in Figure 7. Both GSs have the allylic alcohol situated on the same side of the Ti_2O_2 four-membered ring plane, as indicated by Ti−O−Ti-Oallyl dihedral angles of 114.3° and 97.1° (green bonds, Figure 2a). That both **GS-2a** and **Gs-2b** have a *syn*-configuration is also evidenced by allyl−O-Ti···C−CO_2ET dihedral angles that are nearly parallel (2.4° and −9.5°). The fully loaded Sharpless catalyst has one Ti atom that has a hexacoordinated Ti as a consequence of the bidentate O−O bonding of the peroxide. **GS-2a** has a Ti−O bond to the alcohol of 1.777 Å; the primary Ti−O bond in Ti−O−$OC(CH_3)_3$ is 1.876 Å and is shorter than the secondary η^2-Ti−O bond (2.130 Å). These calculated Ti−O bond distances are in good agreement with a related X-ray study where the two bond distances are 1.913 and 2.269 Å.[32] The allyl alcohol C=C face is ideally poised to receive the transferring oxygen atom in the TS with relatively little heavy atom motion, mainly involving rotation of the C−C bond in the H_2C=CH−CH_2−O-Ti moiety (Figure 7). Only one of the four ester C=O groups has a short Ti···O=C interaction (2.530 Å) that can have a meaningful influence on the overall energetics.

In **GS-2b**, the Ti−O−Ti-Oallyl angle is −117.4°, but the O−C−C=C dihedral angle is −127.4°. Thus, **GS-2b** is also *syn* and yields the 2S-epoxide. The geometry of the peroxide bonds to the Ti is very similar to that in **GS-2a** with the Ti−O peroxide bond at 1.876 Å and the secondary η^2−Ti-O bond being longer (2.209 Å). The O−O bond distance in these ground-state structures is typically ≈1.44 Å. Only one short C=O···Ti interaction (2.418 Å) was found that could markedly influence the total energy or overall geometry. Most importantly, the Gibbs free-energy difference between the two GSs is very small (ΔG = 0.81 kcal/mol), and any difference in barrier heights for the epoxidation step will be a result of electronic factors in the TS. We also located two GS minima with an *anti* relationship of the allyl alcohol with respect to the adjacent CO_2Et group in ring A. **GS-2c** and **GS-2d** are, respectively, 1.62 and 1.00 kcal/mol lower in energy than **GS-2a**. This goes against the long-held assumption that the *syn* GS should be involved in the Sharpless epoxidation of allyl alcohols with smaller substituents on the C=C.[7,33]

Our primary objective in this part of the study is to determine the difference in the Gibbs free energy between the competing epoxidation TSs. The figures describing the TS for the epoxidation are quite congested; insets have been added to point out specific bond lengths and angles. Similar to the ground states, the key dihedral angle between the Ti−O atom of the allyl alcohol and the C−CO_2Et in ring A in the transition states shown in Figure 8 has the two substituents in a parallel orientation (±15°) in the *syn* configuration, while the *anti*-configurations have the allyl alcohol and the CO_2Et moiety opposite each other with a dihedral angle of 110° to 140° (compare with Figure 2). The requisite allyl-O−Ti-C-CO_2Et dihedral angles for **TS-2a** and **TS-2b** (−8.6° and −13.9°) support the *syn* designation, while those for **TS-2c** and **TS-2d** (137.0° and 137.1°) indicate the *anti* designation. For both the *syn* and *anti* configurations of the catalysts, the O−C−C=C dihedral angle in the transition state for allylic alcohol epoxidation is critical for whether the S or the R epoxide prevails in the oxygen atom transfer step.

The O−C−C=C dihedral angle in **TS-2a** is 36.1° and presents the *Si* face of C=C to the transferring oxygen, producing the 2R-epoxide, as predicted by the Sharpless mnemonic[1] (Figure 6). The constraints imposed by the O−C−C=C dihedral angle and the approach of the oxygen not only influence the energetics of the reaction but also impose geometric requirements on the geometry of the TS. The intramolecular oxygen atom transfer to a Ti-bound allylic alcohol in the TS involves addition of the proximal oxygen from the peroxide to the C=C bond with a concomitant 1,3-migration of the *tert*-butoxide ligand to the Ti center. The electrophilic oxygen approaches the midpoint of the C=C π-bond with an angle that is approximately linear (170.5°). The

https://doi.org/10.1021/acs.jpca.3c08476
J. Phys. Chem. A 2024, 128, 2072−2091

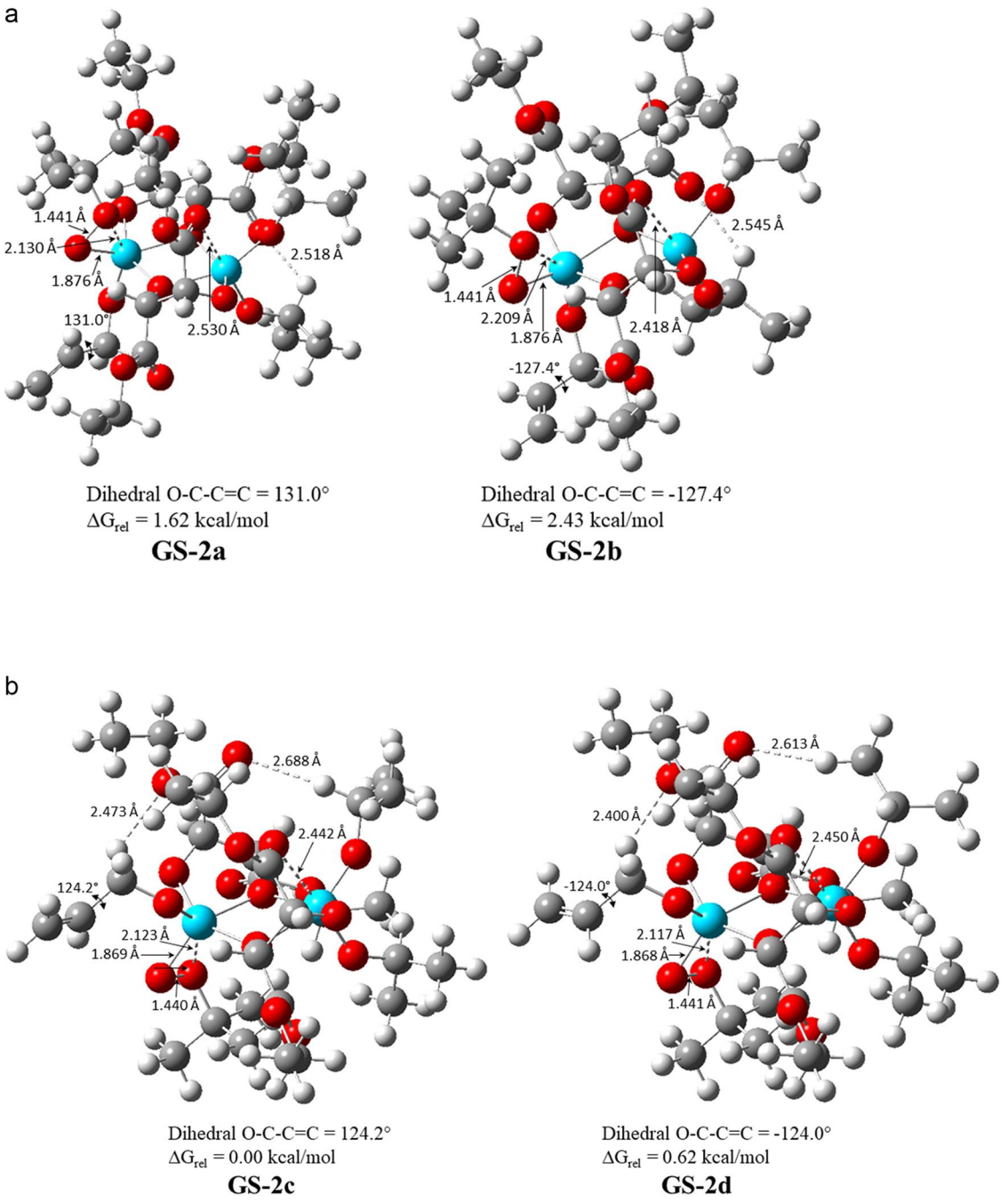

Figure 7. (a) *syn* ground states and (b) *anti* ground states for the epoxidation of allyl alcohol exhibiting the two enantioselective faces of the C═C bond.

O−O bond is elongated from 1.441 Å in **GS-2a** to 1.781 Å in **TS-2a**, and the two Ti−O bonds in the TS are relatively close in length (2.035 and 2.199 Å). The distal *tert*-butoxide is involved in a 1,3-migration to the Ti center, while the proximal oxygen adds to the C═C bond to complete formation of the 3-membered epoxide ring (eq 1). The approach of the transferring oxygen is slightly asymmetric with small differences in the C−O bond distances in the developing epoxide. The angle between the TiOO and COC planes (65.9°) is distorted from 90° for an ideal spiro orientation (angle between planes a and b in Figure 9). The key HOMO−LUMO interactions involving both bond breaking and bond making are also shown. As illustrated in Figure 2, a key stabilizing C═O···Ti interaction is present in ring A (2.526 Å). This *syn* TS has the second lowest activation energy ($\Delta G^{\ddagger}$ = 26.35 kcal/mol).

Epoxidation of the other conformer, **TS-2b**, with a negative O−C−C═C dihedral angle of −106.2°, has the opposite C═C face directed toward the electrophilic oxygen and produces the 2*S*-epoxide. The oxygen is approximately perpendicular to the plane of the C═C bond (101.3° for the angle between the C═CH plane and the TiOO plane) and approaches the midpoint of the C═C bond in a near linearly fashion (175.6°). The incipient C−O epoxide bonds have slightly differing bond distances of 2.024 and 2.154 Å. The O−O bonds in both TSs are elongated to about the same extent (1.800 and 1.781 Å).

https://doi.org/10.1021/acs.jpca.3c08476
J. Phys. Chem. A 2024, 128, 2072−2091

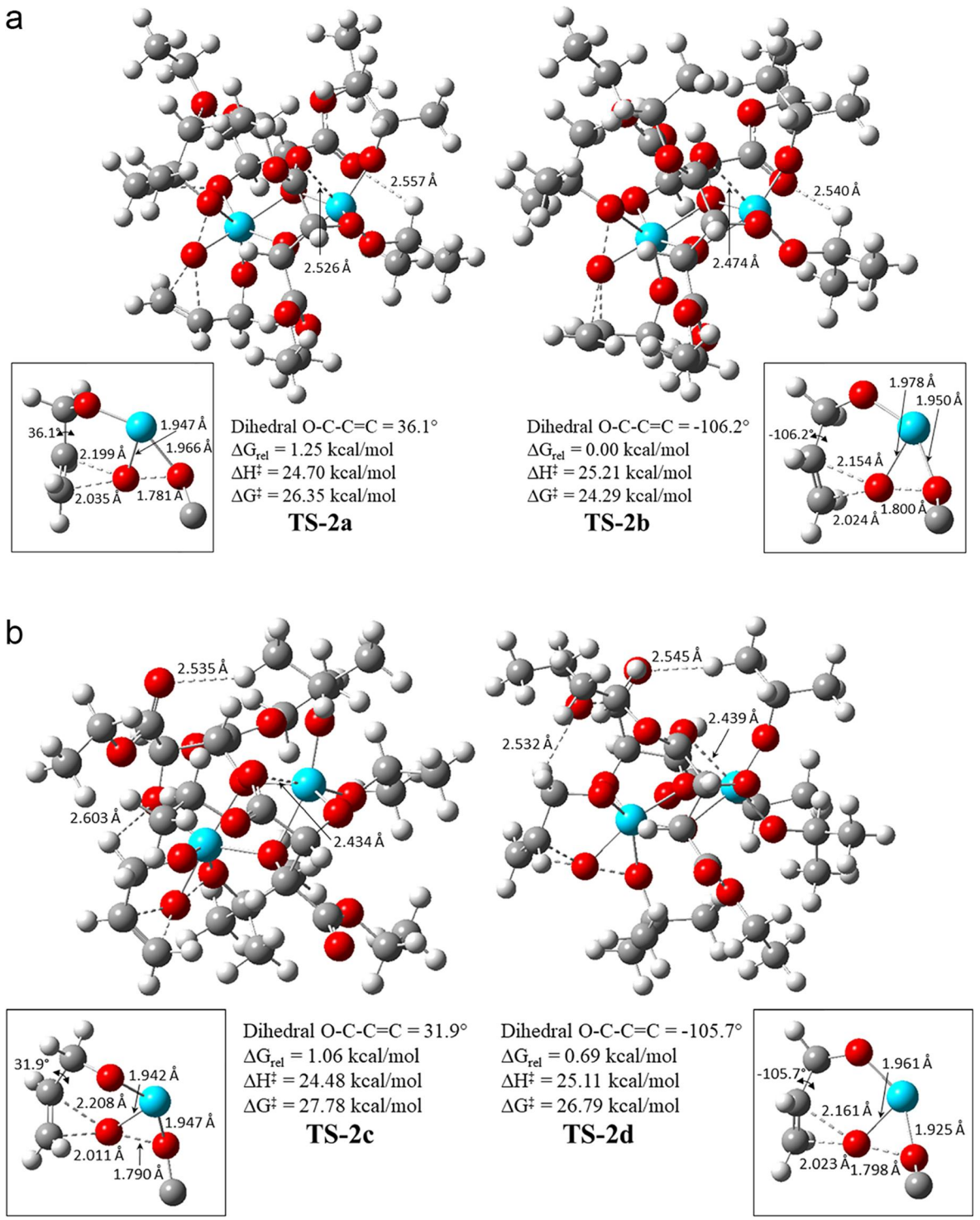

Figure 8. (a) *syn* transition structures for the epoxidation of allyl alcohol exhibiting the two enantioselective faces of the C═C bond. (b) *anti* transition structures for the epoxidation of allyl alcohol exhibiting the two enantioselective faces of the C═C bond.

Both **TS-2a** and **TS-2b** are stabilized by strong C═O···Ti interactions in ring A (2.526 and 2.474 Å, respectively). For **TS-2a** and **TS-2b**, the planes of the R-C═C-R and the Ti−O−O of the Ti(IV) catalyst are nearly perpendicular (101.3° and 96.4°, respectively), thereby maximizing the interaction of the pair of electrons of the incoming electrophilic oxygen atom with the π^* orbital of the alkene. The angle between the TiOO plane and the COC plane of the epoxide product (35.9°) should approach 90° for a pure spiro-TS or near 0° for a planar-TS (Figure 9). This idealized molecular approach is exemplified by comparison with the bimolecular peroxyacetic acid epoxidation of *E*-2-butene as describe above in Figure 4. Even though **TS-2b** is lower in energy, the O−C−C═C dihedral angle (−106.2°) imposes sufficient internal strain to cause **TS-2b** to approach a planar orientation. Despite this, **TS-2b** has the lowest activation barrier of the four TSs examined ($\Delta G^{\ddagger}$ = 24.29 kcal/mol). It is also worthy of note that monomeric pentacoordinate **TS-1** (Figure 5) has a much

https://doi.org/10.1021/acs.jpca.3c08476
J. Phys. Chem. A 2024, 128, 2072−2091

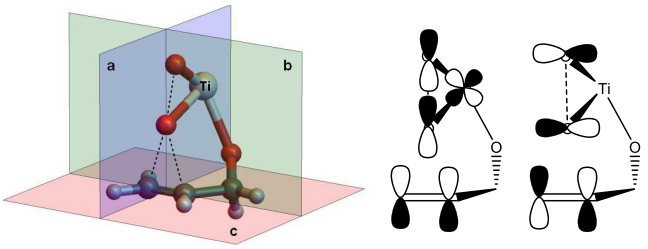

Figure 9. Geometric planes and orbital interactions involved in the spiro orientation for the oxygen transfer step in Ti(IV)-catalyzed epoxidation of allyl alcohol.

greater activation energy than hexacoordinate *syn* **TS-2b** ($\Delta\Delta G^{\ddagger}$ = 6.30 kcal/mol).

Figure 8b shows **TS-2c** and **TS-2d**, the epoxidation transition structures with an *anti* configuration and Ti−O−Oallyl angles of −114.1° and −115.1°. The O−C−C=C dihedral angles are 31.9° for **TS-2c** and −105.7° for **TS-2d**, yielding the R and S epoxides, respectively. The other bond lengths and angles are similar to the corresponding *syn* transition states **TS-2a** and **TS-2b**. Since **TS-2d** is merely 0.36 kcal/mol lower in energy than **TS-3c** (Table 2), only 65% of the product from the *anti* configuration is the preferred 2S-epoxide. In contrast to conventional wisdom, the two GSs with the lowest Gibbs free energy have the *anti* orientation. However, the TS with the lowest $\Delta G^{\ddagger}$ has the anticipated *syn* relationship. Because **TS-2b** is 0.69 kcal/mol lower in energy than **TS-2d**, about 3/4 of the 2S-epoxide comes from the *syn* configuration. The enantiomer excess reflects the degree to which a sample contains one enantiomer in a greater amount than the other (%ee = (R − S)/(R + S) × 100%). Combining the yield from the *syn* and *anti* configurations results in 64.0%ee, which is in modest agreement with the experimentally observed product ratio of 90%ee.[33]

Table 2. Activation Parameters for the GSs and TSs for the Epoxidation of *trans*-Methyl Allyl Alcohol[a]

structure	∠O−C−C=C	Ti−O−Ti-Oallyl dihedral	ΔG_{rel}	$\Delta G^{\ddagger}$ (GS-*n* →TS-*n*)	% epoxide
GS-3a *syn*	136.6	112.8	1.01		
GS-3b *syn*	−122.9	98.6	0.97		
GS-3c *anti*	120.7	−121.2	0.00		
GS-3d *anti*	−120.3	−122.7	3.50		
TS-3a *syn*	42.9	105.5	26.34	25.33	12.1 RR
TS-3b *syn*	−110.3	102.8	25.17	24.20	87.9 SS
TS-3d *anti*	37.6	−112.8	26.51	26.51	26.4 RR
TS-3c *anti*	−110.3	−113.9	25.90	22.40	73.6 SS

[a]For no interconversion between *syn* and *anti*; when *syn*/*anti* interconversion is faster than epoxidation, the calculated yield of the epoxide is 15.8% R,R and 84.2% S,S corresponding to 68.4%ee.

3.5.2. Epoxidation of trans-Methyl Allylic Alcohol. Epoxidation of *trans*-methyl allylic alcohol proved to be more problematic than allylic alcohol itself. The data shown in the above section describing the epoxidation of allyl alcohol is somewhat controversial in that our calculations suggested that the Gibbs free energy of the ground states preferred the *anti*-configuration of the allyl alcohol related to the adjacent CO_2Et group in ring A. For allyl alcohol, we used the default implicit solvent model (IEFPCM) with methylene chloride solvent to remain consistent with the energetics from earlier calculations.[8] To potentially improve the accuracy of the calculations and obtain the correct 2S,3S epoxide in the calculations, we have used the SMD implicit solvation model for the methyl- and *tert*-butyl allyl alcohol epoxidations.

Our objective in this section is to determine the relative Gibbs free energy and orientation of the four possible GSs and TSs for this simplest of *trans* substituted allylic alcohols. We continue to present the catalysts with the *syn* configuration first although we do note that the *anti* loaded catalyst with (*E*)-2-butene-1-ol, **GS-3c** has the lowest energy ground state (Table 2) similar to allyl alcohol, **GS-2c** (see Table 1).

The structures for the ground-state conformers are shown in Figure 10. Conformer **GS-3a** has the alcohol oriented *syn* to the CO_2Et group in ring A and the Ti−O−Ti-Oallyl dihedral angle (green bonds, Figure 2) is 112.8°. The conformation of the O−C−C=C dihedral angle in **GS-3a** is 136.6° and that conformation exposes the *Si* face of the C=C to the electrophilic oxygen to afford the 2R,3R-epoxide in accordance with the Sharpless mnemonic[1] (Figure 6). The O−C−C=C dihedral angle in **GS-3b** is −122.9° and also has a *syn* orientation (Ti−O−Ti-Oallyl dihedral angle of 98.6°) but exposes the *Re* face. The Ti−O bond to the allylic alcohol is 1.765 Å and the primary Ti−O bond in Ti−O−$OC(CH_3)_3$ is 1.875 Å and as expected is shorter than the secondary η^2-Ti−O bond (2.208 Å). Conformer **GS-3b** is only 0.045 kcal/mol lower in energy than **GS-3a** and has essentially the same geometric parameters as **GS-3a** (Figure 10a). The other two conformers, **GS-3c** and **GS-3d**, have O−C−C=C dihedral angles of 120.7° and −120.3°, respectively; Ti−O−Ti-Oallyl dihedral angles of −121.2° and −122.7° indicate that they have an *anti* configuration. However, **GS-3d** is 3.5 kcal/mol higher in energy than **GS-3c**.

The four related methyl-allyl epoxidation TSs are shown in Figure 11 and exhibit similar trends in structure and energetics compared to allyl alcohol. The *syn* **TS-3b** and *anti* **TS-3d** are lower in energy than their corresponding *syn* **TS-3a** and *anti* **TS-3c** (Table 2). **TS-3a** has a positive O−C−C=C dihedral angle of (42.9°) and a Ti−O−Oallyl angle (105.5°) placing it on the same side of the Ti_2O_2 plane as the adjacent CO_2Et group in the A ring, confirming its *syn* configuration that affords the 2R,3R-epoxide. The insets in Figure 11a detail the geometry of the oxygen transfer step. The developing C−O epoxide bonds in **TS-3a** are 2.082 and 2.191 Å and the C=C bond distance (1.356 Å) is only slightly elongated from its GS geometry (1.330 Å). The allylic alcohol Ti−O bond (1.817 Å) and the transferring oxygen Ti−O bond (1.944 Å) form a OTiO angle of 89.5°. In **TS-3a**, only one relatively strong C=O bonding interaction with a Ti atom is noted (C=O···Ti = 2.514 Å) with another such interaction being very much weaker (3.429).

In **TS-3b**, the O−C−C=C dihedral angle of −110.3° affords the opposite enantiomer, the 2S,3S epoxide. The O−O bond has increased from 1.441 to 1.798 Å in the transition state and the Ti−O-allyl bond is 1.812 Å. The Ti-peroxide bond is 1.966 Å and the secondary η^2−Ti-O bond is about the same at 1.954 Å attending the 1,3-migration of the $OC(CH_3)_3$ ligand to the Ti atom. The developing C−O bonds are typical for this type of oxidation process, as shown in the inset in

https://doi.org/10.1021/acs.jpca.3c08476
J. Phys. Chem. A 2024, 128, 2072−2091

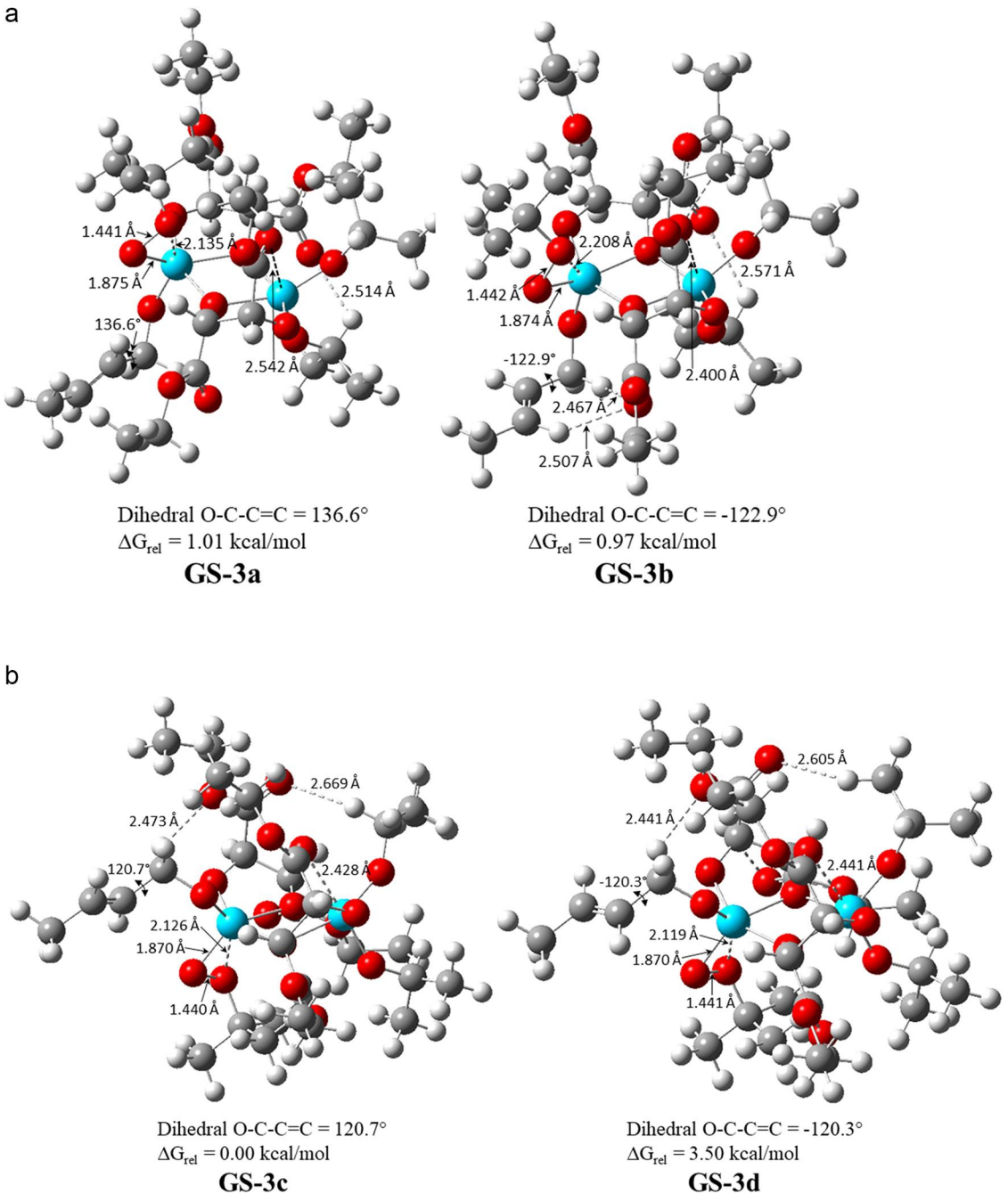

Figure 10. (a) *syn* ground-state structures for the epoxidation of *trans*-methyl allyl alcohol exhibiting the two enantioselective faces of the C═C bond. (b) *anti* ground-state structures for the epoxidation of *trans*-methyl allyl alcohol exhibiting the two enantioselective faces of the C═C bond.

Figure 11a. The overall conformations of the CO_2Et groups are about the same as in **TS-3a**, and again, we observe only one strong C═O···Ti interaction (2.491 Å). This TS has one H-bond where the allyl alcohol itself is bound to a C═O group (2.322 Å) with several additional H-bonds to the O-*i*-Pr CH_3 groups. The free energy of activation for **TS-3b** ($\Delta G^{\ddagger}$ = 24.20 kcal/mol) is 1.13 kcal/mol lower than that for **TS-3a**.

The approach of the electrophilic oxygen to the midpoint of C═C in **TS-3a** and **TS-3b** is nearly linear (171.9° and 171.0°, respectively). The C═C/TiOO planes are nearly orthogonal (84.2° and 89.0°, respectively), and the angles between the COC and TiOO planes are 65.2° and 36.2°, respectively. Even though **TS-3b** has a lower Gibbs free energy, this TS has an orientation approaching planar, similar to **TS-2b**. However, *anti* **TS-3d** has the lowest activation barrier ($\Delta G^{\ddagger}$ = 22.4 kcal/mol), and this is 1.89 kcal/mol lower than the lowest $\Delta G^{\ddagger}$ for epoxidation of allyl alcohol (Table 1). The *syn* transition structure with the negative O−C−C═C dihedral angle (**TS-3b**) is consistent with conventional wisdom in that the major epoxide product has the 2S,3S absolute configuration (87.9%, Table 2) which corresponds to 75.8% ee.

The transitions states for epoxidation with the *anti* "loaded" catalysts, **TS-3c** and **TS-3d**, are shown in Figure 11b and have Ti−O−Oallyl angles of −112.8° and −113.9°, respectively. The other geometric parameters are similar to the corresponding *syn* conformers. The difference in Gibbs free energy for **TS-3c** and **TS-3d** ($\Delta\Delta G$ = 0.61 kcal/mol, Table 2) indicates that only 70% of the product from the *anti* configuration is the

https://doi.org/10.1021/acs.jpca.3c08476
J. Phys. Chem. A 2024, 128, 2072−2091

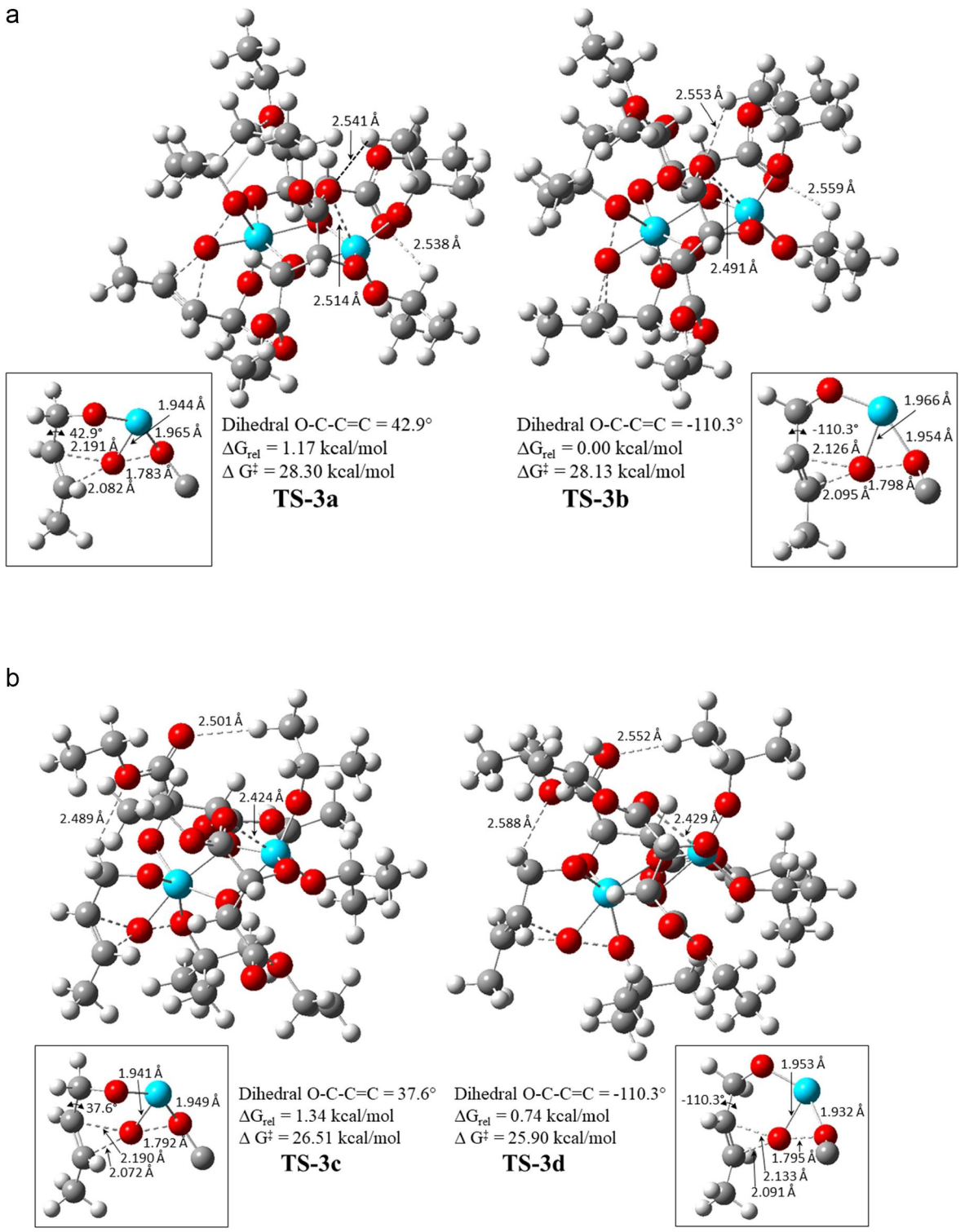

Figure 11. (a) *syn* transition structures for the epoxidation of *trans*-methyl allyl alcohol exhibiting the two enantioselective faces of the C═C bond. (b) *anti* transition structures for the epoxidation of *trans*-methyl allyl alcohol exhibiting the two enantioselective faces of the C═C bond.

anticipated 2S,3S-epoxide. Because **TS-3d** is 0.73 kcal/mol higher in energy than **TS-3b**, about 23% of the 2S,3S-epoxide comes from the *anti* configuration. The combined yield from the *syn* and *anti* configurations has 68.4%ee.

3.5.3. Epoxidation of trans-tert-Butyl Allylic Alcohol. It was generally assumed that there have been no cases reported showing that the C═C face selection for the asymmetric epoxidation of a prochiral allylic alcohol varies from that predicted by the Sharpless mnemonic[1] provided in Figure 6. This concept was rigorously tested by substituting a sterically demanding *tert*-butyl group at each of the C−H positions of allylic alcohol. In each case, the results supported a consistent enantiofacial selection producing the predicted 2S,3S-epoxide.[39] These data showed that the *trans-tert*-butyl substituent imposed the least steric inhibition, while substitution at the *cis* position presented the greatest. In this part of the study, we

https://doi.org/10.1021/acs.jpca.3c08476
J. Phys. Chem. A 2024, 128, 2072−2091

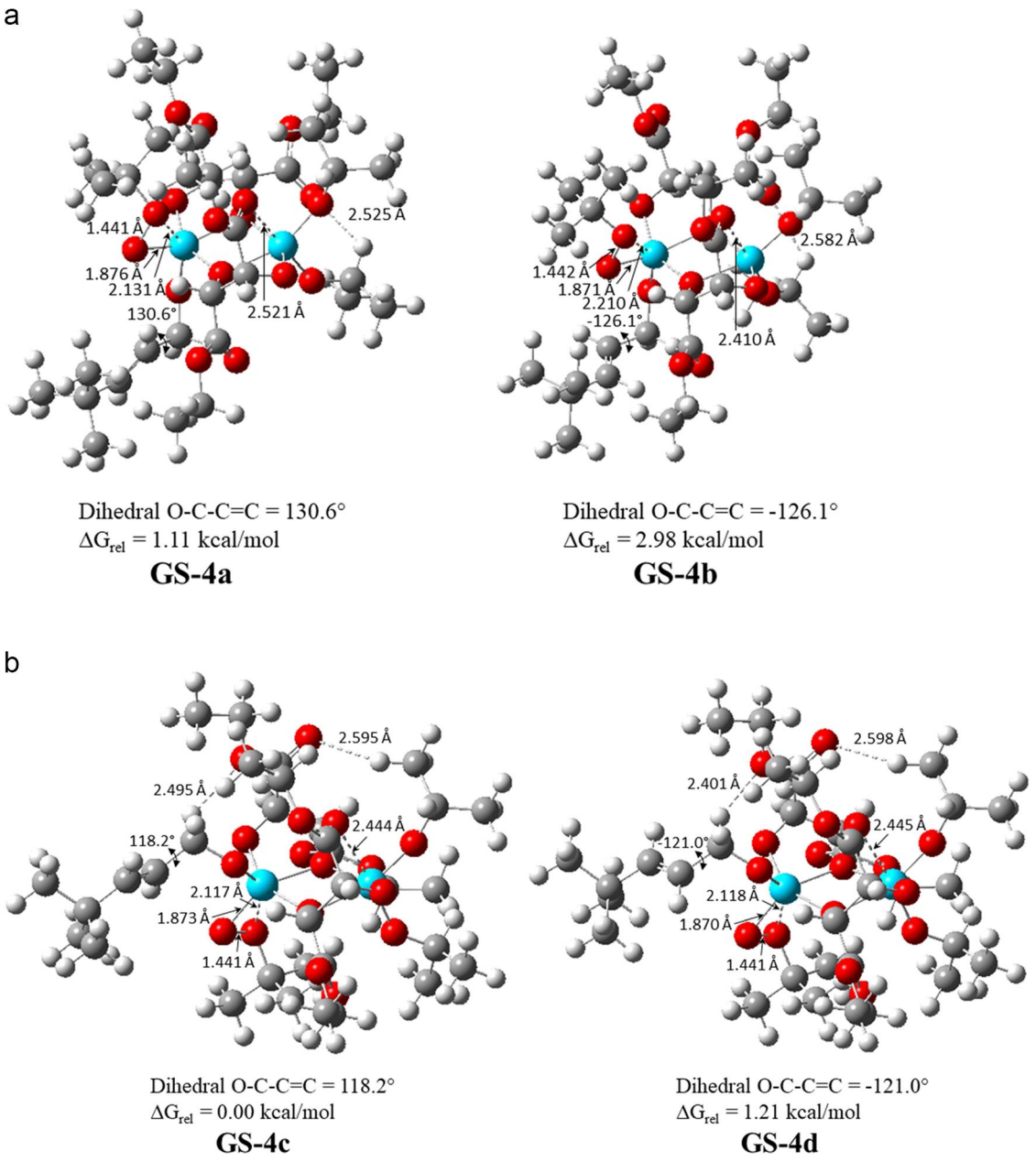

Figure 12. (a) *syn* ground states for the epoxidation of *trans-tert*-butyl alcohol exhibiting the two enantioselective faces of the C═C bond. (b) *anti* ground states for the epoxidation of *trans-tert*-butyl alcohol exhibiting the two enantioselective faces of the C═C bond.

examine the enantioselectivity of the epoxidation of the *trans-tert*-butyl allylic alcohol. As noted above, it is also often just assumed that the incoming allyl alcohol will adopt the *syn* conformation, so we start our examination from that perspective.

The orientation of the allylic alcohol in both **GS-4a** and **GS-4b** is *syn* to CO_2Et in ring A, while **GS-4c** and **GS-4d** are *anti* to CO_2Et in ring A (Figure 12). The Ti−O−Ti-Oallyl dihedral angles in **GS-4a** and **GS-4b** (112.4° and 100.5°, respectively) confirm that the allyl group is *syn* to the adjacent CO_2Et in the A ring, as portrayed in Figure 2. **GS-4a** with the positive O−C−C═C dihedral angle (130.6°) is 1.87 kcal/mol lower in Gibbs free energy than **GS-4b** with the negative dihedral angle (−126.1°), which would provide the desired 2S,3S-epoxide product. In both cases, the allyl alcohol *tert-butyl* group resides out and away from the bulk of the very sterically encumbered Ti-tartrate catalyst. Both GSs have an important stabilizing C═O···Ti interaction, (2.521 and 2.410 Å). As noted above, we have estimated that a C═O···Ti bonding interaction can contribute a stabilization of ≈14 kcal/mol, compared to ≈10 kcal/mol for EtO···Ti interactions (see Figure 3). The magnitude of this interaction will obviously be influenced by the local steric environment and how close the CO_2Et group can get to the Ti center. Each GS also has a number of relatively short stabilizing O···H hydrogen bonds (<2.6 Å). Recall, we have also shown that the developing O···Ti oxygen interaction along the reaction coordinate in epoxide product formation can markedly influence the total energy (≈12 kcal/mol)[11] and exothermicity of the epoxidation reaction.

The transition states are shown in Figure 13. Both of the TSs in Figure 13a have the same *syn* orientation of the allylic alcohol relative to the adjacent CO_2Et group as their respective

https://doi.org/10.1021/acs.jpca.3c08476
J. Phys. Chem. A 2024, 128, 2072−2091

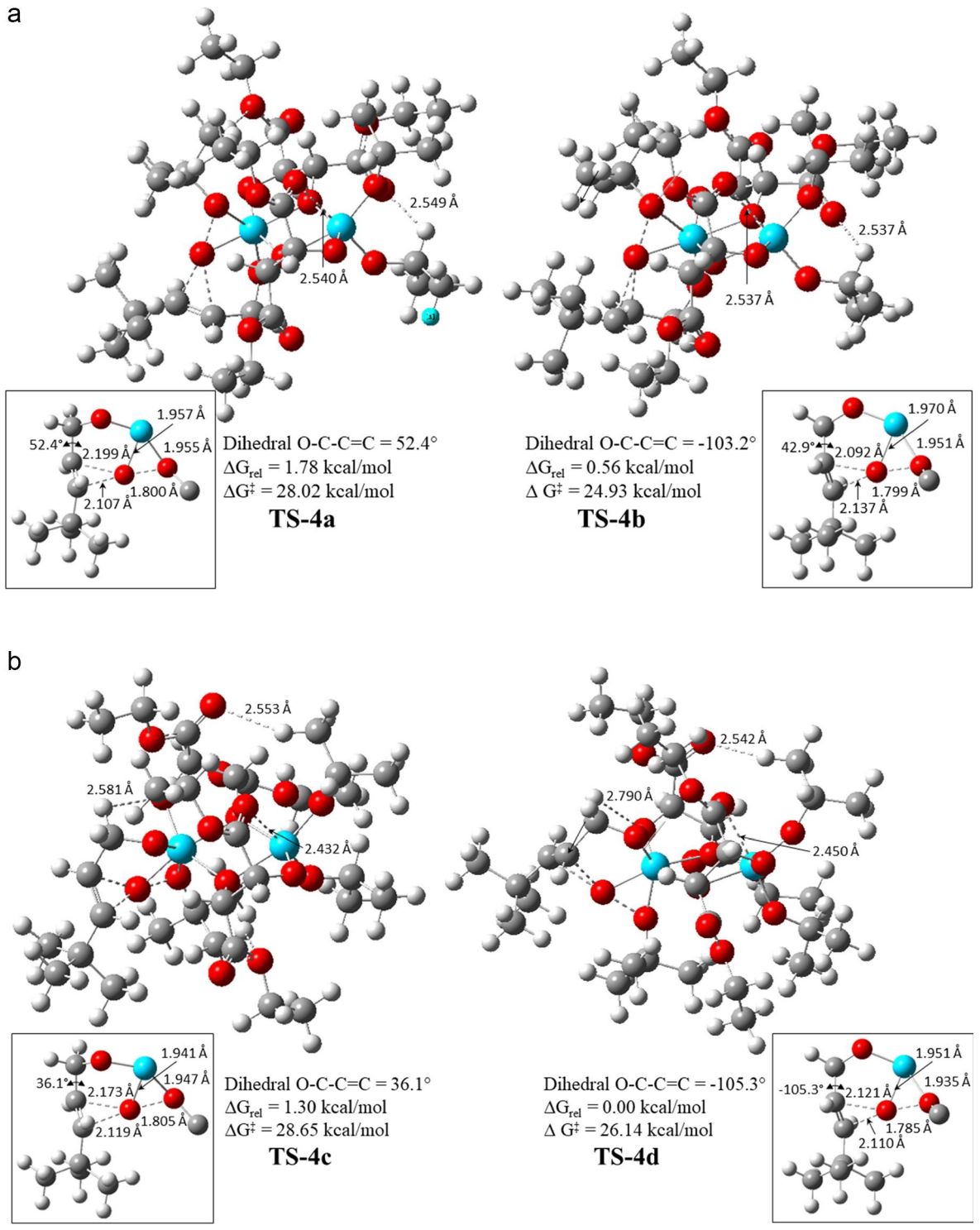

Figure 13. (a) *syn* transition states for the epoxidation of *trans-tert*-butyl alcohol exhibiting the two enantioselective faces of the C═C bond. (b) *anti* transition states for the epoxidation of *trans-tert*-butyl alcohol exhibiting the two enantioselective faces of the C═C bond.

GSs (**GS-4a** and **GS-4b**). The O−C−C═C dihedral angle for **TS-4a** (52.4°) has the transferring oxygen poised to produce the oxirane ring in the 2R,3R-epoxide as it approached the center of the C═C bond at an angle of 171.1°. The activation energy for **TS-4a**, relative to its corresponding GS that also has a positive dihedral angle, is $\Delta G^{\ddagger}$ = 28.02 kcal/mol. This activation barrier is higher than that calculated for the less sterically hindered *trans*-methyl-allyl alcohol ($\Delta G^{\ddagger}$ = 25.33 kcal/mol). In **TS-4b**, which has a O−C−C═C dihedral angle of −103.2°, the electrophilic oxygen approached C═C in close to linear (174.8°) and the angle between the C═CH and TiOO planes is essentially perpendicular (90.5°).

The angle between the C−O−C and TiOO planes (48.8°) deviates significantly from the ideal spiro angle of 90°. The $\Delta G^{\ddagger}$ = 24.93 kcal/mol for **TS-4b** differs from **TS-4a** by 3.09 kcal/mol. Despite this relatively large difference in $\Delta G^{\ddagger}$, the difference in Gibbs free energy of the two TSs is only 1.22

https://doi.org/10.1021/acs.jpca.3c08476
J. Phys. Chem. A 2024, 128, 2072−2091

kcal/mol, indicating that the 2S,3S-epoxide is favored by 88.8% (Table 3).

Table 3. Activation Parameters for the Epoxidation of *trans-tert*-Butyl Allyl Alcohol

structure	∠O−C−C=C	Ti−O−Ti-Oallyl dihedral	ΔG_{rel}	$\Delta G^{\ddagger}$ (GS-*n* →TS-*n*)	% epoxide[a]
GS-4a *syn*	130.6	112.4	1.11		
GS-4b *syn*	−126.1	100.5	2.98		
GS-4c *anti*	118.2	−122.3	0.00		
GS-4d *anti*	−121.0	−123.1	1.21		
TS-4a *syn*	52.4	105.1	29.13	28.02	11.2% R,R
TS-4b *syn*	−103.2	104.9	27.91	24.93	88.8% S,S
TS-4c *anti*	36.1	−116.9	28.65	28.65	10.0% R,R
TS-4d *anti*	−105.3	−117.4	27.35	26.14	90.0% S,S

[a]For no interconversion between *syn* and *anti*; when *syn*/*anti* interconversion is faster than epoxidation, the calculated yield of the epoxide is 10.4% R,R and 89.6% S,S corresponding to 79.2%ee.

Next, we examined the relative free energies of the *anti* GSs versus the *syn* GSs for the *trans*-substituted allyl alcohols because of the obvious steric interactions imposed by the *tert*-butyl group. **GS-4c** has a Gibbs free energy 1.21 kcal/mol higher than **GS-4d** that has a negative O−C−C=C dihedral angle of −121.0° (Figure 12b). Both **GS-4c** and **GS-4d** have the oxygen atom of the allyl alcohol on the same side of the plane of the Ti_2O_2 4-membered ring (out-of-plane angle of −50.8° and −50.0°) and are in the *anti* configuration (Figure 12b). More to the point, however, *anti* **GS-4c** is 1.11 kcal/mol lower in Gibbs free energy than its corresponding syn **GS-4a** (Table 3). The *anti* configuration transition state, **TS-4c** (Figure 13b), has a Gibbs free energy that is 0.48 kcal/mol lower than *syn* **TS-4a** that also has a positive O−C−C=C dihedral angle (Table 1). **TS-4d** is 0.56 kcal/mol lower than **TS-4b** and has a negative O−C−C=C dihedral angle.

The four TSs examined are all relatively close in Gibbs free energy (ΔΔ*G* = 1.78 kcal/mol). Each TS has an important stabilizing C=O···Ti bonding interaction (2.43 to 2.54 Å). The lowest energy TS, *anti* **TS-4d**, has an O−C−C=C dihedral angle −105.3° and a Ti−O−Ti-Oallyl angle of −117.4° (Figure 13b). The O−O bond approaches the midpoint of the C=C bond at an angle of 172.3° and has an angle between the C=CH and TiOO planes of 86.2°. However, again we see that the angle between the planes of the developing epoxide (C−O−C) and the TiOO plane in **TS-4d** (56.6°) has experienced sufficient torsion that it has deviated significantly from a pure spiro-TS orientation. The two developing C−O bonds have the typical bond lengths of ≈2.1 Å, and the O−O bond distance has elongated to 1.785 Å. The migrating $OC(CH_3)_3$ ligand has a Ti−O bond distance of 1.935 Å, and the proximal Ti−O bond had a comparable distance of 1.951 Å attending the 1,3-rearrangement of the peroxide. We also see a number of O···H secondary bonds that have obviously contributed to its lower Gibbs free energy. We observe six H-bonding interactions that are less than 2.6 Å.

The competing *anti* **TS-4c** has fewer H-bonding interactions than **TS-4d** and is 1.3 kcal/mol higher in energy. This TS produces the 2R,3R-epoxide and has a positive a O−C−C=C dihedral angle (36.1°) and a Ti−O−Ti-allyl angle of −116.9° (Figure 13b). The O−O bond has an angle with the C=C midpoint that approaches linearity (170.4°) and the TiOO angle between the C=CH and TiOO planes is 89.1°. The angles between the C−O−C and TiOO planes in **TS-4c** and **TS-4d** (68.3° and 56.6°, respectively) are not sufficiently different to provide an explanation for the energy difference between these two *anti* TSs. It is noteworthy that we generally observe that a positive O−C−C=C dihedral angle typically results in a TS that is closer to a spiro approach but that does not appear to provide an explanation for the difference in orientation of approach.

The most important observation that we have made is that **TS-4d**, with an *anti* configuration and a negative O−C−C=C dihedral angle (−105.3°), provides the predicted 2S,3S-epoxide and has a Gibbs free energy that is 1.3 kcal/mol lower than corresponding *anti* **TS-4c**. Experimental data report[39] a 52% yield for this reaction, which did not proceed to completion, but gave a > 95% ee. The calculated activation

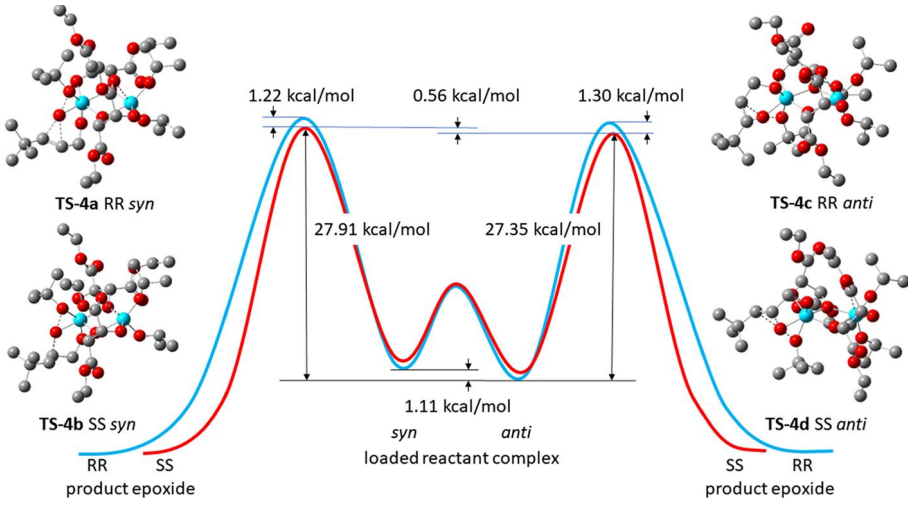

Figure 14. Curtin−Hammett analysis of the Gibbs free energy of epoxidation of *syn* and *anti* catalyst conformations for *trans-tert*-butyl allyl alcohol.

https://doi.org/10.1021/acs.jpca.3c08476
J. Phys. Chem. A 2024, 128, 2072−2091

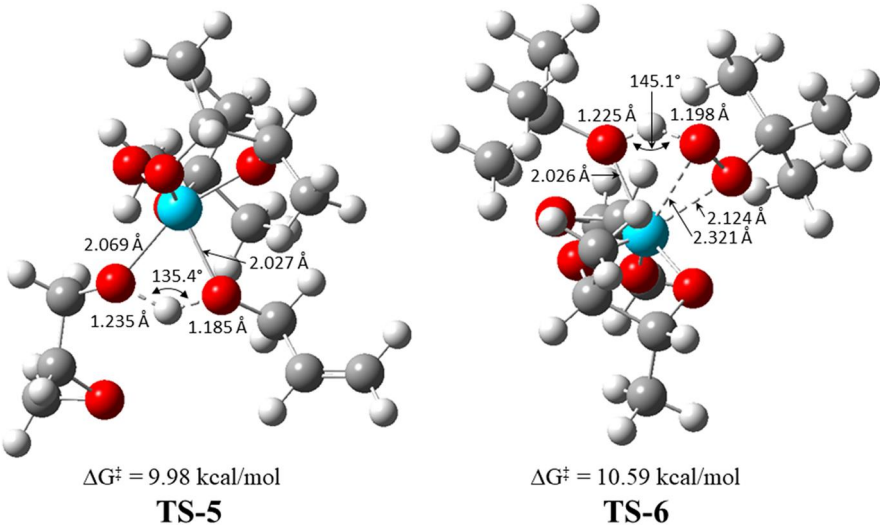

Figure 15. Transition structures for ligand exchange of allyl alcohol with the epoxide product (**TS-5**) and *tert*-butyl hydroperoxide exchange with the *tert*-butyl oxide anion (**TS-6**) to regenerate the loaded catalyst.

barrier for **TS-4d** ($\Delta G^{\ddagger}$ = 26.14 kcal/mol) cannot be directly compared to an experimental value. Finn has reported[40] a value of $\Delta H^{\ddagger}$ = 10.6 kcal/mol for the epoxidation of cyclohexyl methyl carbinol (1-methyl-2-cyclohexen-1-ol), but this barrier includes the equilibrium constants (K_1K_2) for both allyl alcohol and peroxide exchange with HO-*i*-Pr prior to the oxidation step.[41] The ground-state structures with the *syn* orientation, **GS-4a** and **GS-4b**, should be able to interconvert readily via rotation about the O−C−C═C dihedral angle. Likewise, the *anti* structures, **GS-4c** and **GS-4d**, should also be able to interconvert rapidly. The most stable *anti* structure, **GS-4c**, is 1.11 kcal/mol lower in energy than the most stable *syn* structure, **GS-4a**. The potential energy profiles for C_2-C_3 bond rotation in allylic alcohols show that the rotational energy barriers are typically very low. In an earlier study, we reported that the C−C rotational barrier for the interconversion of two equilibrating conformers of Ti-bound allyl alcohols is $\Delta G^{\ddagger}$ = 4.11 kcal/mol.[11] However, it was also noted that methyl substituents can increase this rotational barrier by 3−4 kcal/mol. By comparison, the individual barriers for the formation of the epoxides are 25−29 kcal/mol. These data strongly suggest that the barriers for the conversion between the four different ground-state structures are estimated to be significantly lower than the barriers for the formation of the epoxide products. Thus, the Curtin−Hammett principle[42] applies, and the ratio of the S,S versus R,R products is determined by the relative energy of the four transition states (see Figure 14). Similar plots can be constructed for allyl and methyl-allyl alcohol epoxidation.

The two lowest energy transition states, **TS-4b** and **TS-4d** (27.91 and 27.35 kcal/mol, respectively, relative to **GS-4c**), produce the 2S,3S epoxide, while **TS-4a** and **TS-4c** are higher in energy (29.13 and 28.65 kcal/mol, respectively) and produce the R,R epoxide. Combining the results for all 4 transition states yields 89.6% S,S epoxide and 10.4% R,R epoxide. This corresponds to a calculated 79.2% ee, in reasonable agreement with the experimental estimate of 95% ee.[39]

3.6. Ligand Exchange Mechanism for Catalyst Regeneration. One of the basic tenets of a catalytic epoxidation reaction is that the product of the initial epoxidation must be rapidly exchanged in situ with the substrate allylic alcohol in order to regenerate the loaded catalyst and repeat the catalytic cycle. In this section, we demonstrate that the activation barriers that facilitate such rapid ligand exchange are much lower than the epoxidation barriers. In our earlier study[11] on Ti(IV)-catalyzed epoxidation, we showed that when our model reactant Ti(O-*i*-Pr)$_2$CH$_3$OOH(OCH$_2$CH$_2$O) undergoes exchange of its O-*i*-Pr alkoxide ligand with methyl hydroperoxide (CH_3OOH), the activation barrier was $\Delta G^{\ddagger}$ = 4.00 kcal/mol when measured from a prereaction GS complex but $\Delta G^{\ddagger}$ = 6.73 kcal/mol from isolated reactants.[11] The prereaction complex for the ligand exchange TS basically consists of CH_3COOH hydrogen bonding to the oxygen atom of the incipient O-*i*-Pr leaving group with a relatively strong H-bond. Similarly, we found that the ligand exchange involving *tert*-butyl hydroperoxide also has a relatively low Gibbs free energy of activation $\Delta G^{\ddagger}$ = 6.15 kcal/mol and the overall Gibbs free energy of exchange was slightly negative (ΔG = −2.59 kcal/mol). In the present study, for our model Ti(IV) catalyst, we have added two methyl groups of 2R,3R-butane diol to provide an abbreviated approximation for the 2R,3R diethyl tartrate present in the Sharpless catalyst. The epoxidation product and the transition states for ligand exchange are shown in Figure 15.

The first step in regenerating the loaded catalyst is the displacement of the epoxy alcoholate by allyl alcohol (**TS-5**). This assumption is based upon the fact that the substrate allyl alcohol is typically present in a 20-fold excess relative to the catalyst.[43] The transition state for exchange has a barrier of $\Delta G^{\ddagger}$ = 9.98 kcal/mol and involves a proton transfer between allyl alcohol and the epoxide alcohol. **TS-5** has elongated O−H bond distances (1.235 and 1.185 Å) and a large imaginary frequency (ν_i = 1251.2i cm^{-1}). The transition vector indicates that atom motion in the TS is essentially the proton transferring between the two adjacent oxygen atoms. The Ti−O bonds made and broken in the TS are nearly equal in length (2.069 Å vs 2.027 Å) with the bond to the leaving epoxy alcohol being slightly longer. The transferring proton also interacts with the Ti atom (2.157 Å).

The TS for exchange of $(CH_3)_3COOH$ for $CH_3)_3CO^-$ is similar, consisting almost entirely of the proton from

https://doi.org/10.1021/acs.jpca.3c08476
J. Phys. Chem. A 2024, 128, 2072−2091

$(CH_3)_3CO-OH$ migrating to the Ti−O-*tert*-butyl oxygen (**TS-6**). The migrating proton is approximately halfway between the two oxygens (1.225 and 1.198 Å) and is attended by a very large imaginary frequency (ν_i = 1053.9i cm^{-1}) consistent with light atom movement. Initially, we had anticipated a ligand exchange reaction involving an addition to the Ti center, with displacement of the protonated departing ligand. Instead, we observe a TS that is largely involved with proton transfer from the incoming hydroperoxide OH group to the departing *tert*-butyl alcohol. The Gibbs free energy barrier for **TS-6**, $\Delta G^{\ddagger}$ = 10.59 kcal/mol, is similar to the displacement of the epoxy alcoholate by allyl alcohol, **TS-5**.

As noted above, experimental data for the $\Delta G^{\ddagger}$ of exchange of isopropoxide with isopropanol has been reported to be ≈14−15 kcal/mol.[5] We also note that the Gibbs free energy activation barriers herein are measured from isolated reactions, and we would anticipate that these energies should be several kcal/mol higher if consideration is given to the H-bonding interactions in a prereaction GS. These data place our calculated $\Delta G^{\ddagger}$ in very good agreement with values measured in solution.[5]

Modification of the original Sharpless procedure,[33] which allowed the asymmetric epoxidation to be carried out with just 5−10% catalyst, removed any doubt about the efficacy of the rapid reversible ligand exchange that repeats the catalytic cycle. The experimental catalyst reaction mixture[43] typically had a 20-fold excess of allylic alcohol substrate to the catalytic Ti(IV) reagent, Ti(O-i-Pr)$_4$, but yields of epoxide can be produced in greater than 90% yield with >90% ee. This requires very efficient ligand exchange with limited side reactions. However, the possibility for nonproductive ligand exchange also exists such as exchange of a $(CH_3)_3CO-OH$ for the epoxy alcohol, instead of a $(CH_3)_3CO^-$. This exchange reaction has the same low activation barrier, $\Delta G^{\ddagger}$ = 10.38 kcal/mol, and also has the potential to correct an errant exchange and still regenerate the required loaded catalyst. We have shown that the predicted 2S,3S-epoxide can be derived from either the *syn* or *anti* catalyst as long as the allylic alcohol has a negative O−C−C=C dihedral angle. Thus, with the low $\Delta G^{\ddagger}$ values for exchange, a statistical mixture of ligands results, including both *syn* or *anti* loaded catalysts with both an allylic alcohol and a TBHP juxtaposed in the proper orientation to allow epoxidation to occur.

4. NOTE OF CAUTION

Finally, we wish to address the method in which the enantiomeric is actually measured experimentally. The enantiomeric excess (% ee) reported for the Sharpless epoxidation is typically based upon either NMR analysis with a chiral reagent in solution on the crude product or gas chromatography data based upon a suitable derivative in solution. However, in selected cases when the epoxide product is purified by recrystallization and the % ee is measured on the isolated product, the results may be less reliable because of the potential for separation of one of the stereoisomers, especially when the crude product is an oil. A case in point is the epoxidation of *trans*-phenyl allylic alcohol where the crude product ((2*S*,3*S*)-3-phenyloxirane-2-yl) methanol was purified by recrystallization from petroleum ether (mp 51−53 °C) before the %ee was measured. In one case, the reported %ee was 90% ee,[4] and in another, it was >98% ee.[33] However, our extended efforts failed to corroborate these experimental data and suggested that the enantioselectivity for *trans*-phenyl allylic alcohol, with its planar phenyl group protruding out and away from the chiral centers of the catalyst, may be closer to a 50/50 isomer ratio than the much greater values reported. We suggest that this experiment could warrant closer investigation.

5. SUMMARY

5.1. Dimerization of the Monomeric Catalyst. A systematic study of the mechanistic pathways for the Sharpless epoxidation reaction has shown that the Ti(IV)-catalyzed epoxidation proceeds by an entirely different mechanism from classical peroxyacid epoxidation of alkenes and hydrocarbon oxidation with alkyl hydroperoxides. A mixture of electronic and steric factors is responsible for the overall success of this rather remarkable epoxidation reaction. The first step in the overall epoxidation process is the formation of a dimeric Ti(IV) chiral tartrate complex. The considerable driving force (ΔG = −34.27 kcal/mol) for the dimerization of tetracoordinate monomeric Ti(IV) catalyst is a consequence of the greater thermodynamic stability of pentacoordinate Ti dimer. A Ti center with a pentacoordinate environment also results in a more reactive Ti(IV) epoxidation catalyst than a tetracoordinate catalyst ($\Delta\Delta G^{\ddagger}$ = 7.54 kcal/mol).

5.2. Formation of the "Loaded Catalyst". Formation of the effective loaded Sharpless catalyst involves rapid and reversible ligand exchange of the O-*i*-Pr ligands with the substrate allyl alcohol and the *tert*-butyl alkyl hydroperoxide. Both exchanges occur with small barriers ($\Delta G^{\ddagger}$ = 10 kcal/mol) that are substantially lower than the epoxidation barriers ($\Delta G^{\ddagger}$ = 24−29 kcal/mol). The motion in the TS for both exchanges is essentially the proton transferring between the two adjacent oxygen atoms. In the loaded catalyst, one of the four CO_2Et groups of chiral tartaric ester of the dimeric catalyst forms a strong C=O···Ti interaction (ca. 14 kcal/mol) that markedly influences the overall relative stability of the loaded catalyst and serves to restrain the molecular motion in ring A.

5.3. Oxygen Transfer Step. The molecular motion in the Ti(IV)-catalyzed epoxidation involves a 1,3 rearrangement of the *tert*-butyl group with the oxygen proximal to Ti transferred to the alkene substrate. The Ti-bound allylic alcohol with a negative O−C−C=C dihedral angle produces the 2S,3S-epoxide, while a positive O−C−C=C dihedral angle in the TS yields the 2R,3R-epoxide.

For the *trans*-methyl allyl alcohol, the *syn* and *anti* transition states for the S,S-epoxide are, respectively, 1.33 and 0.61 kcal/mol lower than for the R,R-epoxide. By the Curtin−Hammett principle, the difference in the four transition state free energies yields the 2S,3S-epoxide in 68.4%ee, in modest agreement with experiment.[33]

The activation barriers for the epoxidation *trans-tert*-butyl allylic alcohol are about 2 kcal/mol higher with that for the less sterically hindered *trans*-methyl-allyl alcohol. The *syn* and *anti* transition states for the S,S-epoxide are, respectively, 1.78 and 1.30 kcal/mol lower than for the R,R-epoxide. Combining the results for all 4 transition states yields 89.6% S,S epoxide and 10.4% R,R epoxide. This corresponds to a calculated 79.2%ee, in reasonable agreement with the experimental estimate of 95% ee.

■ ASSOCIATED CONTENT

Supporting Information

The Supporting Information is available free of charge at https://pubs.acs.org/doi/10.1021/acs.jpca.3c08476.

https://doi.org/10.1021/acs.jpca.3c08476
J. Phys. Chem. A 2024, 128, 2072−2091

Total energies and Cartesian coordinates for all structures (PDF)

AUTHOR INFORMATION

Corresponding Author

Robert D. Bach − *Department of Chemistry and Biochemistry, University of Delaware, Newark, Delaware 19716, United States;* orcid.org/0000-0002-7331-5279; Email: rbach@udel.edu

Author

H. Bernhard Schlegel − *Department of Chemistry, Wayne State University, Detroit, Michigan 48202, United States;* orcid.org/0000-0001-7114-2821

Complete contact information is available at: https://pubs.acs.org/10.1021/acs.jpca.3c08476

Notes

The authors declare no competing financial interest.

ACKNOWLEDGMENTS

This work was supported in part by a grant from the National Science Foundation (CHE1856437) to H.B.S. SEAGrid (http:www.seagrid.org) is acknowledged for computational resources and services for the selected results used in this publication. This work used the Extreme Science and Engineering Discovery Environment (XSEDE), which is supported by National Science Foundation grant number OCI-1053575. We are particularly thankful to Dr. Sudhakar Pamidighantam for his assistance with the calculations carried out at SEAGRID.[44,45]

REFERENCES

(1) Katsuki, T.; Sharpless, K. B. The First Practical Method for Asymmetric Epoxidation. *J. Am. Chem. Soc.* **1980**, *102*, 5974−5976.

(2) Johnson, R. A.; Sharpless, K. B. In *Comprehensive Organic Synthesis*; Trost, B. M.; Fleming, I., Eds.; Pergamon Press: New York, 1991; vol 7; pp 389−436.

(3) Sharpless, K. B.; Woodard, S. S. On The Mechanism of Titanium-Tartrate Catalyzed Asymmetric Epoxidation. *Pure Appl. Chem.* **1983**, *55*, 1823−1836.

(4) Guo, H.-C.; Shi, X.-Y.; Wang, X.; Liu, S.-Z.; Wang, M. Liquid-Phase Synthesis of Chiral Tartrate Ligand Library for Enantioselective Sharpless Epoxidation of Allylic Alcohols. *J. Org. Chem.* **2004**, *69*, 2042−2047.

(5) Finn, M. G.; Sharpless, K. B. Mechanism of Asymmetric Epoxidation. 2. Catalyst Structure. *J. Am. Chem. Soc.* **1991**, *113*, 113−126.

(6) Willams, I. D.; Pedersen, S. F.; Sharpless, K. B.; Lippard, S. J. Crystal-Structures of 2 Titanium Tartrate Asymmetric Epoxidation Catalysts. *J. Am. Chem. Soc.* **1984**, *106*, 6430−6431.

(7) Sharpless, K. B. Searching for New Reactivity (Nobel Lecture). *Angew. Chem., Int. Ed.* **2002**, *41*, 2024−2032.

(8) Bach, R. D. Structure and Mechanism for Alkane Oxidation and Alkene Epoxidation with Hydroperoxides, α-Hydroxy Peroxides and Peroxyacids. A Theoretical Study. *J. Phys. Chem. A* **2019**, *123*, 9520−9530.

(9) Bach, R. D.; Schlegel, H. B. Bond Dissociation Energy of Peroxides Revisited. *J. Phys. Chem. A* **2020**, *124*, 4742−4751.

(10) Chong, A. O.; Sharpless, K. B. On the Mechanism of the Molybdenum and Vanadium Catalyzed Epoxidation of Olefins by Alkyl Hydroperoxides. *J. Org. Chem.* **1977**, *42*, 1587−1590.

(11) Bach, R. D.; Schlegel, H. B. Mechanism of Orbital Interactions in the Sharpless Epoxidation with Ti(IV) Peroxides. A DFT Study. *J. Phys. Chem. A* **2021**, *125*, 10541−10556.

(12) Frisch, M. J.; Trucks, G. W.; Schlegel, H. B.; Scuseria, G. E.; Robb, M. A.; Cheeseman, J. R.; Scalmani, G.; Barone, V.; Mennucci, B.; Petersson, G. *Gaussian 16, revision B.01*; Gaussian, Inc.: Wallingford, CT, 2019.

(13) Schlegel, H. B. Geometry Optimization. *WIREs Comput. Mol. Sci.* **2011**, *1*, 780−809.

(14) Zhao, Y.; Truhlar, D. G. The M06 Suite of Density Functionals for Main Group Thermochemistry, Thermochemical Kinetics, Noncovalent Interactions, Excited States, and Transition Elements: Two New Functionals and Systematic Testing of Four M06-Class Functionals and 12 Other Functionals. *Theor. Chem. Acc.* **2008**, *120*, 215−241.

(15) Becke, A. D. Density-Functional Exchange-Energy Approximation with Correct Asymptotic Behavior. *Phys. Rev. A* **1988**, *38*, 3098−3100.

(16) Becke, A. D. Density - Functional Thermochemistry. III. The Role of Exact Exchange. *J. Chem. Phys.* **1993**, *98*, 5648−5652.

(17) Bach, R. D.; Schlegel, H. B. The Bond Dissociation Energy of the N-O Bond. *J. Phys. Chem. A* **2021**, *125*, 5014−5021.

(18) Zhao, Y.; Schultz, N. E.; Truhlar, D. G. Design of Density Functionals by Combining the Method of Constraint Satisfaction with Parametrization for Thermochemistry, Thermochemical Kinetics, and Noncovalent Interactions. *J. Chem. Theory Comput.* **2006**, *2*, 364−382.

(19) Marenich, A. V.; Cramer, C. J.; Truhlar, D. J. Universal Model on Solute Electron Density and on a Continuum Model of the Solvent Defined by the Bulk Dielectric Constant and Atomic Surface Tensions. *J. Phys. Chem. B* **2009**, *113* (18), 6378−6396.

(20) Montgomery, J. A.; Frisch, M. J.; Ochterski, J. W.; Petersson, G. A. A Complete Basis Set Model Chemistry. VII. Use of the Minimum Population Localization Method. *J. Chem. Phys.* **2000**, *112*, 6532−6542.

(21) Ochterski, J. W.; Petersson, G. A.; Montgomery, J. A., Jr A Complete Basis Set Model Chemistry. V. Extensions to Six or More Heavy Atoms. *J. Chem. Phys.* **1996**, *104*, 2598−2619.

(22) Jorgensen, K. A.; Wheeler, R. A.; Hoffman, R. Electronic and Steric Factors Determining the Asymmetric Epoxidation of Allylic Alcohols by Titanium-Tartrate Complexes (The Sharpless Epoxidation). *J. Am. Chem. Soc.* **1987**, *109*, 3241−3246.

(23) Wu, Y. D.; Lai, D. K. W. A Density Functional Study on the Stereocontrol of the Sharpless Epoxidation. *J. Am. Chem. Soc.* **1995**, *117*, 11327−11336.

(24) Wu, Y. D.; Lai, D. K. W. Transition Structure for the Epoxidation Mediated by Titanium(IV) Peroxide. A Density Functional Study. *J. Org. Chem.* **1995**, *60*, 673−680.

(25) Sever, R. R.; Root, T. W. DFT Study of Solvent Coordination Effects on Titanium-Based Epoxidation Catalysts. Part Two: Reactivity of Titanium Hydroperoxo Complexes in Ethylene Epoxidation. *J. Phys. Chem. B* **2003**, *107*, 4090−4099.

(26) Antonova, N. S.; Carbo, J. J.; Kortz, U.; Kholdeeva, O. A.; Poblet, J. M. Mechanistic Insights into Alkene Epoxidation with H_2O_2 by Ti- and other TM-Containing Polyoxometalates: Role of the Metal Nature and Coordination Environment. *J. Am. Chem. Soc.* **2010**, *132*, 7488−7497.

(27) Jimenez-Lozano, P.; Ivanchikova, I. D.; Kholdeeva, O. A.; Poblet, J. M. Alkene Epoxidation by Ti-Containing Polyoxometalates. Unambiguous Characterization of the Role of the Protonation State. *Chem. Commun.* **2012**, *48*, 9266−9268.

(28) Jimenez-Lozano, P.; Skobelev, I. Y.; Kholdeeva, O. A.; Poblet, J. M.; Carbo, J. J. Epoxidation Catalyzed by Ti-Containing Polyoxometalates: Unprecedented β-Oxygen Transfer Mechanism. *Inorg. Chem.* **2016**, *55*, 6080−6084.

(29) Cui, M.; Adam, W.; Shen, J. H.; Luo, X. M.; Tan, X. J.; Chen, K. X.; Ji, R. Y.; Jiang, H. J. A Density-Functional Study of the Mechanism for the Diastereoselective Epoxidation of Chiral Allylic Alcohols by the Titanium Peroxy Complexes. *J. Org. Chem.* **2002**, *67*, 1427−1435.

(30) Freindorf, M.; Kraka, E. Mechanistic Details of the Sharpless Epoxidation of Allylic Alcohols—A Combined URVA and Local Mode Study. *Catalysts* **2022**, *12*, 789−820.

(31) Fernandes, A. S.; Maitre, P.; Correra, T. C. Evaluation of the Katsuki-Sharpless Epoxidation Precatalysts by ESI-FTMS, CID, and IRMPD Spectroscopy. *J. Phys. Chem. A* **2019**, *123*, 1022−1029.
(32) Boche, G.; Mobus, K.; Harms, K.; Marsch, M. [(η^2-tert-Butylperoxo)titanatrane)$_2$. 3 Dichloromethane]: X-ray Crystal Structure and Oxidation Reactions. *J. Am. Chem. Soc.* **1996**, *118*, 2770−2771.
(33) Gao, Y.; Hanson, R. M.; Klunder, J. M.; Ko, S. Y.; Masamune, H.; Sharpless, K. B. Catalytic Asymmetric Epoxidation and Kinetic Resolution: Modified Procedures Including *in situ* Derivatization. *J. Am. Chem. Soc.* **1987**, *109*, 5765−5779.
(34) Bach, R. D.; Wolber, J. G.; Coddens, B. A. On the Mechanism of Metal-Catalyzed Epoxidation. A Model for the Bonding in Peroxo-Metal Complexes. *J. Am. Chem. Soc.* **1984**, *106*, 6098−6099.
(35) Bach, R. D.; Dmitrenko, O. Spiro versus Planar Structures in the Epoxidation of Simple Alkenes. A Reassessment of the Level of Theory Required. *J. Phys. Chem. A* **2003**, *107*, 4300−4306.
(36) Singleton, D. A.; Merrigan, S. R.; Liu, J.; Houk, K. N. Experimental Geometry of the Epoxidation Transition State. *J. Am. Chem.* **1997**, *119*, 3385−3386.
(37) Jorgensen, K. A. Transition-Metal-Catalyzed Epoxidation. *Chem. Rev.* **1989**, *89*, 431−457.
(38) Bach, R. D.; Winter, J. E.; Estevez, C. M. On the Origin of Substrate Directing Effects in the Epoxidation of Allylic Alcohol with Peroxyformic Acid. *J. Am. Chem. Soc.* **1998**, *120*, 680−685.
(39) Schweiter, M. J.; Sharpless, K. B. *Tetrahedron Lett.* **1985**, *26*, 2543−2546.
(40) Finn, M. G. On the Mechanism of Titanium-Tartrate Catalyzed Asymmetric Epoxidation. PhD Thesis. Massachusetts Institute of Technology, 1985; p 41.
(41) McKee, B. H.; Kalantar, T. H.; Sharpless, K. B. Subtle Effects in the Asymmetric Epoxidation: Dependence of Kinetic Efficiency on the Monodentate Alkoxide Ligands of the ByStander Titanium Center. *J. Org. Chem.* **1991**, *56*, 6966−6968.
(42) Seeman, J. J. The Curtin-Hammett Principle and the Winstein-Holness Kinetics. *J. Chem. Educ.* **1986**, *63*, 42−48.
(43) In a typical experimental procedure[33] for carrying out asymmetric epoxidation with only a catalytic amount of Ti(O-i-Pr)$_4$, 6.0 mmol (1.2 equiv) of diethyl tartrate were cooled in a solution of methylene chloride before addition of (5mmol (1.0 equiv) of Ti(O-i-Pr)$_4$. The reaction mixture was stirred (−20 °C) and 200 mmol of TBHP was added to initiate the exchange reaction. After 30 min 100 mmol of (E2)-2-octanol over a period of 20 min and stirred for 20 min at −20 °C. The excess TBHP was quenched with a ferrous sulfate/tartaric acid workup that gave 88% crude yield of epoxide at 92.3% ee.
(44) Pamidighantam, S.; Nakandala, S.; Abeysinghe, E.; Wimalasena, C.; Yodage, S. R.; Marru, S.; Pierce, M. Community Science Exemplars in SEAGrid Science Gateway: Apache Airavata Based Implementation of Advanced Infrastructure. *Procedia Comput. Sci.* **2016**, *80*, 1927−1939.
(45) Shen, N.; Fan, Y.; Pamidighantam, S. E-Science Infrastructures for Molecular Modeling and Parametrization. *J. Comput. Sci.* **2014**, *5*, 576−589.

https://doi.org/10.1021/acs.jpca.3c08476
J. Phys. Chem. A 2024, 128, 2072−2091